A Novel Non-Apoptotic Role for Caspase Activity during Cardiac Hypertrophy

Rebecca Leigh Stiles

Thesis submitted to the
Faculty of Graduate and Postdoctoral Studies
In partial fulfillment of the requirements
For the MSc degree in Cellular and Molecular Medicine.

Department of Cellular and Molecular Medicine
Faculty of Medicine
University of Ottawa

Abstract

Cardiac hypertrophy is an adaptive response in which the heart grows in size to normalize output during times of cardiac stress or increased demand. This increase in heart mass originates from the growth of individual cardiomyocytes rather than cellular division. Many of the cellular modifications and cytoskeletal reorganization that occurs during hypertrophy is reminiscent of apoptosis. Members of the caspase family have been well characterized for their role in apoptosis, and have recently been implicated in cardiac differentiation, as well as skeletal muscle differentiation and immune cell development. Recent studies have reported that inhibition of caspase-3 activity limited the ability of the heart to undergo pathological hypertrophy *in vivo*, suggesting a role for caspase-3 in the hypertrophic growth process. It remains to be seen whether or not the effect in the heart is cell autonomous, what caspase proteins are involved, and how caspases are eliciting their effect within the cell. Data presented here indicate that inhibition of caspase-3 and caspase-8 minimizes hypertrophic growth in a primary neonatal rat ventricular cardiomyocyte cell model. Treatment with hypertrophic agonist phenylephrine induced an approximate 45% increase in cell size after 24 hours which was attenuated with the addition of caspase inhibitors. These data suggest that caspase-3 and caspase-8 may be involved in hypertrophic growth of cardiomyocytes. Furthermore, results suggest that a uniform increase in caspase activity may not be directly responsible for the observed effect. Rather, that subcellular localization of the caspase proteases may contribute to the effects seen during hypertrophy.

Table of Contents

List of Tables

List of Figures

List of Abbreviations

AMC	7-amino-4-methylcoumarin
ANF	Atrial natriuretic factor
Ang II	Angiotensin II
Apaf-1	Apoptosis activating factor 1
BIR	Baculovirus IAP repeat
BNP	B-type natriuretic factor
BSA	Bovine Serum Albumin
CAD	Caspase activated DNase
CaMK	Calcium/calmodulin-dependent protein kinase
CAR	Coxsackie–adenovirus receptors
CARD	Caspase recruitment domain
Caspase	Cysteinyl-aspartate specific protease
cDNA	Complementary Deoxyribonucleic acid
CFP	Cyan fluorescent protein
DAG	Diacylglycerol
DAPI	4,6-Diamidino-2-phenylindole
DED	Death effector domain
DEPC	Diethylpyrocarbonate
DMEM	Dulbecco's modified Eagle medium media
DNA	Deoxyribonucleic acid
ECC	Excitation-contraction coupling
EDTA	Ethylenediaminetetraacetic acid
ER	Endoplasmic reticulum
ERK	Extracellular signal-regulated kinase
ET-1	Endothelin 1
FADD	Fas associated death domain
FBS	Fetal Bovine Serum
FLICA	Fluorescent labeled inhibitor of caspases
FMK	Fluoromethylketone
FRET	Fluorescence resonant energy transfer
GAPDH	Glyceraldehyde-3-phosphate dehydrogenase
GFP	Green fluorescent protein
GPCR	G protein-coupled receptor
HDAC	Histone deacetylase
HF	Heart failure
IAP	Inhibitor of apoptosis
ICAD	Inhibitor of caspase activated DNase
IGF-1	Insulin growth factor-1
IgG	Immunoglobulin G
IL-1$_\beta$	Interleukin 1-β
J-MEM	Joklik's Modified Eagle's Medium
JNK	Janus kinase
LV	Left ventricle
MAPK	Mitogen activated protein kinase

Mef2	Myocyte enhancer factor 2
MEK	MAP or ERK kinase
MHC	Myosin heavy chain
MI	Myocardial infarction
NFAT	Nuclear factor of activated T-cells
NF-*k*B	Nuclear factor kappa B
PAAC	Partial abdominal aortic constriction
PARP	Poly (ADP-ribose) polymerase.
PBS	Phosphate buffered saline
PCR	Polymerase chain reaction
PE	Phenylephrine
PFA	Paraformaldehyde
PI3K	Phosphotidylinositol-3-OH kinase
RNA	Ribonucleic acid
ROS	Reactive oxygen species
RSL	Reactive site loop
RT-PCR	Reverse-transcriptase-polymerase chain reaction
SCAT	Spatio-temporal activation of caspases
SF	Serum-free
TNF	Tumor necrosis factor
YFP	Yellow fluorescent protein

Acknowledgements

I would like to sincerely thank my supervisor, Dr. Lynn Megeney, for his mentorship, and for allowing me the opportunity to study in such an exciting environment, as well as my committee members, Dr. Rashmi Kothary and Dr. Valerie Wallace, for their guidance and insight throughout this project. Thank you to the current and former members of the Megeney Lab who have helped me along the way; from brainstorming to trouble-shooting, you are all amazing and this experience would not have been the same without you. I would also like to thank my family and friends who have supported me. Your encouragement, as well as your patience, has meant so much to me.

Rebecca Stiles

CHAPTER 1

Introduction

1.1 Cardiac Physiology

The developing organism requires a continuous supply of oxygenated blood. To meet this demand, the heart is amongst the first organs to develop during embryogenesis (Olson, 2006). Heart development is orchestrated by a number of cardiac specific, evolutionarily conserved genes and transcription factors including GATA4, MEF2 and Nkx2.5**.** In mammalian cardiogenesis, the formation of the heart is initiated by a crescent of mesodermal precursor cells that have been committed to the cardiac lineage. These cells develop into a linear heart tube which is comprised of an inner endocardium and surrounded by myocardium which produces the contractile force (Anton *et al*., 2007). Following development of the linear heart tube, this structure undergoes a process known as cardiac looping which arranges the four chambers of the mammalian heart in the proper orientation (Srivastava and Olson, 2000; Sucov, 1998). This process is further illustrated in Figure 1.

The mammalian cardiovascular system has evolved from that of the fish, which consisted of a two chambered heart; to a three chambered heart common to amphibians such as the mud puppy to finally produce a four-chambered heart consisting of two atrial and two ventricular chambers (Olson, 2006). This system allows for more efficient transport of oxygenated blood as the pulmonary and systemic circulatory systems remain separated within the heart. Specifically, the right atrium receives deoxygenated blood from the body; the blood then travels through the atrioventricular valve, or semi-lunar tricuspid valve, to the right

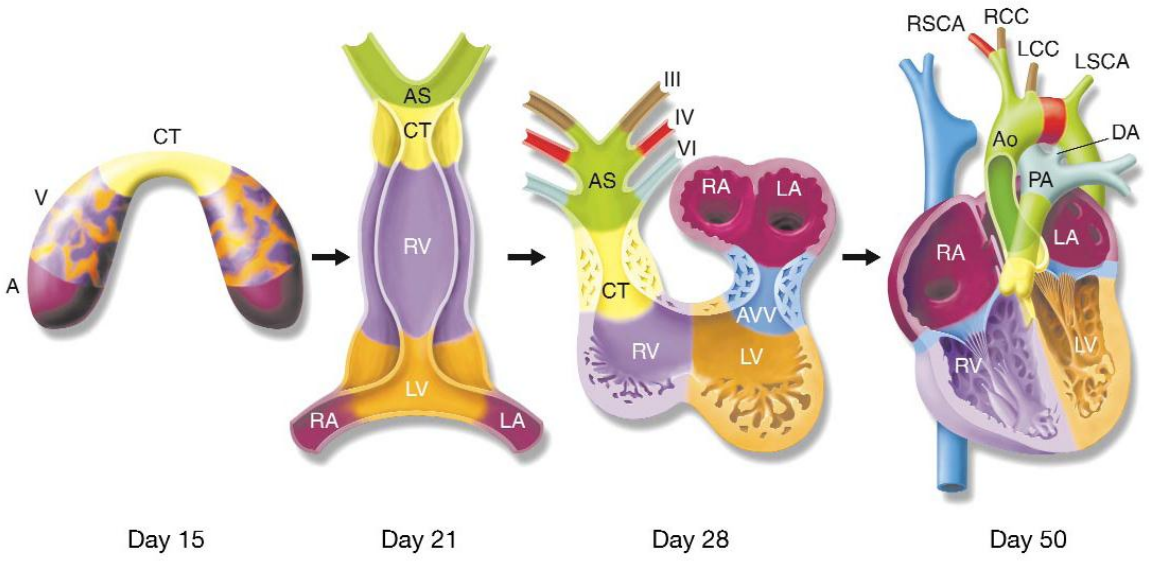

Figure 1: Depiction of cardiac development in *Homo sapiens*; The mammalian heart initially forms from a crescent of precursor cells, into a linear heart tube, then undergoes a process of cardiac looping to finally produce a four chambered heart in the proper orientation. [CT, conotruncal; V, ventricle; A, atrium; AS, aortic sac; RV, right venricle; LV, left ventricle; RA, right atrium; LA, left atrium; AVV, atrioventricular valve; RSCA, right subclavian artery; RCC, right common carotid; LCC, left common carotid; LSCA, left subclavian artery; DA, ductus arteriosus; A_0, aorta; PA, pulmonary artery]. (Reprinted by permission from Macmillan Publishers Ltd: Nature 407(6802):221-228, 2000.)

ventricle and through the pulmonary artery to the lungs where it receives oxygen and releases carbon dioxide through the process of diffusion. Upon returning to the left atrium, oxygenated blood travels through the mitral valve to the left ventricle, which pumps the oxygenated blood through the aorta, to the rest of the body. As described, this heart physiology maintains separation of oxygenated and deoxygenated blood and consequently allows for increased energy expenditure and higher metabolic potential.

The contractile function of the heart stems largely from the presence of cardiac myocytes, which are a type of specialized muscle cell, comprised of myofibrils with repeating sarcomeric units (McMullen and Jennings, 2007; Gregorio and Antin, 2000). Although the cardiomyocyte population comprises the largest mass and volume of the heart, they only make up approximately 30% of the total cell number; smooth muscle cells, endothelial cells and fibroblasts contribute to the remaining, heterogeneous cell population within the organ (Souders *et al*., 2009; McMullen and Jennings, 2007). Additionally, depending on the stimulus, macrophages, mast cells and lymphocytes may also be present in the heart (Banerjee *et al*., 2006). During conditions such as cardiac hypertrophy, when the heart is stimulated to increase in size, the growth is a result of an increase in the size of individual cardiomyocytes rather than the other disparate cell types.

1.2 Cardiac Hypertrophy

Cardiac hypertrophy is an adaptive response in which the heart increases in size in order to maintain cardiac output during times of stress. When the heart is placed under unusual conditions, in the form of systemic hypertension, myocardial infarction (MI), endurance exercise, or pregnancy, hypertrophy may occur as a compensatory response. Cardiac hypertrophy is associated with an increase in the size of individual cardiomyocytes. As cardiomyocytes are terminally differentiated, the compensatory growth that occurs during hypertrophy originates from an expansion in the size of the existing cells rather than hyperplasia per se (McMullen and Jennings, 2007). Thickening of the ventricular wall allows the heart to temporarily normalize wall stress and cardiac output. Depending on the type of cardiac hypertrophy occurring, the consequences of this growth can vary significantly; from enhanced cardiac function, to cardiac dilation and heart failure, the latter being the leading cause of mortality in the Western world (Wehrens *et al*., 2005; Heineke and Molkentin, 2006). Figure 2 outlines several additional phenotypic characteristics associated with the two distinct forms of cardiac hypertrophy.

1.2.1 Physiological Hypertrophy

Physiological hypertrophy may be induced by stimuli such as extensive endurance exercise or pregnancy (Hill and Olson, 2008). This form of hypertrophy also occurs naturally during post-natal heart growth and development (Zak, 1973). Under these circumstances, the heart responds to the increased requirement for pumping oxygenated blood to either the muscles or a

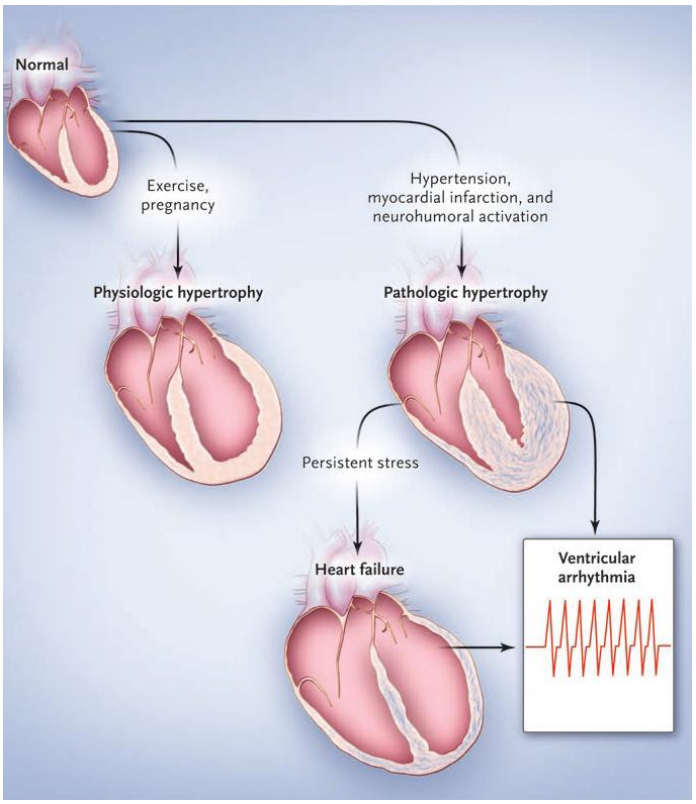

Figure 2: Overview of pathological and physiological cardiac hypertrophy. Depending on the stimulus, cardiac hypertrophy may be either physiological as indicated by normal sarcomeric organization and a matched increase in chamber size, or pathological, which can eventually lead to heart failure. (Reprinted by permission from the Massachusetts Medical Society: NEJM 358(13):1370-1380, 2008.)

developing fetus by hypertrophy of cardiac myocytes. In the case of physiological hypertrophy, growth occurs while maintaining the normal organization of the sarcomere (McMullen and Jennings, 2007). Reflective of these stimuli, the phenotypic changes in heart morphology are reversible upon removal of the stimulus and associated load.

In an animal model, physiological hypertrophy can be induced through chronic swim training. The resulting hypertrophied heart exhibits an increased volume of cardiomyocytes as well as the formation of new sarcomeres, accompanied by an increase in protein synthesis. This form of hypertrophy is typically demonstrated by a matched increase in ventricular wall thickness and chamber dimension. Physiological hypertrophy can arise from either aerobic exercise, or weight training, which typically results in eccentric or concentric cardiac hypertrophy, respectively. Eccentric hypertrophy occurs when sarcomeres are added in series, resulting in an increase in the overall length of the cardiomyocytes. In contrast, concentric hypertrophy results from the addition of sarcomeres in parallel, causing an increase in the cross-sectional area of the cardiomyocytes (Heineke and Molkentin, 2006; Barry and Townsend, 2010). Both eccentric and concentric hypertrophy are also seen in the pathological heart, (see section 1.2.2), however the matched increase in chamber dimension is unique to the physiological setting.

Although the signaling pathways involved in physiological hypertrophy have not been entirely elucidated, Insulin Growth Factor 1 (IGF-1) and

phosphoinositide-3 Kinase (PI3-K) have emerged as key factors (McMullen *et al*., 2003; Dorn, 2007; McMullen *et al*., 2007). IGF-1 was shown to be increased in serum levels of athletes experiencing physiological cardiac hypertrophy (Vitale *et al*., 2008; McMullen *et al*., 2007), implicating the involvement of IGF-1 in this signaling. Additionally, transgenic animal models have confirmed that enhanced IGF-1 signaling results in cardiac hypertrophy without affecting life span; furthermore, blocking aspects of the IGF-1 pathway have been found to blunt cardiac hypertrophy induced by chronic swim training, but not pressure overload, indicating that IGF-1 is involved in physiological but not pathological cardiac hypertrophy (McMullen *et al*., 2003).

1.2.2 Pathological Hypertrophy

Pathological cardiac hypertrophy may arise in response to numerous stimuli such as myocardial infarction (MI), hypertension, valve disease, and genetic mutations (McMullen and Jennings, 2007; Barry and Townsend, 2010). As discussed previously, pathological hypertrophy is also associated with an increase in myocyte volume, sarcomere formation and protein translation (McMullen and Jennings, 2007; Heineke and Molkentin, 2006). However, in the case of pathological hypertrophy, growth of the cardiomyocytes may produce a situation in which the increase in ventricular mass is not matched with an increase in ventricular chamber size (Heineke and Molkentin, 2006). Hypertension is known to cause pressure overload within the heart, which produces a concentric form of hypertrophic growth in which the cardiomyocytes of the left ventricle increase in parallel to produce a thickening of the ventricular

wall (Barry and Townsend, 2010). Alternatively, volume overload, as seen in individuals with mitral valve disorders, produces eccentric hypertrophy. With continued stress, the ventricular wall may experience a form of dilation; here the myocardium begins to thin, leading eventually to heart failure (Hill and Olson, 2008).

In contrast to physiological hypertrophy, there are numerous molecular differences associated with the pathological hypertrophic process. For example, cardiomyocytes begin to re-express fetal genes such as atrial natriuretic factor (ANF), brain natriuretic peptide (BNP) and the β-isoform of Myosin Heavy Chain (β-MHC). The re-expression of ANF and BNP is followed by their secretion from the hypertrophic heart. These proteins are then able to initiate diuresis and vasodilation, which subsequently lowers blood pressure and helps to regulate blood volume (Hall, 2004; Kuhn *et al*., 2002; Horio *et al*., 2000).

As in physiological hypertrophy, the molecular pathways involved in pathological cardiac hypertrophy have not been completely elucidated; however Figure 3 outlines some of the key players identified as being involved in the two forms of hypertrophic signaling. Agonists such as Angiotensin II (AngII), Endothelin I (ET-1) and Phenylephrine (PE) signal through G-Protein Coupled Receptors (GPCRs); upon activation of the receptor, the subunits of the G protein are able to dissociate and activate downstream intracellular signaling pathways (Frey and Olson, 2003). Signaling through $G_{q/11}$ results in the activation of phospholipase C which signals through diacylglycerol (DAG) and

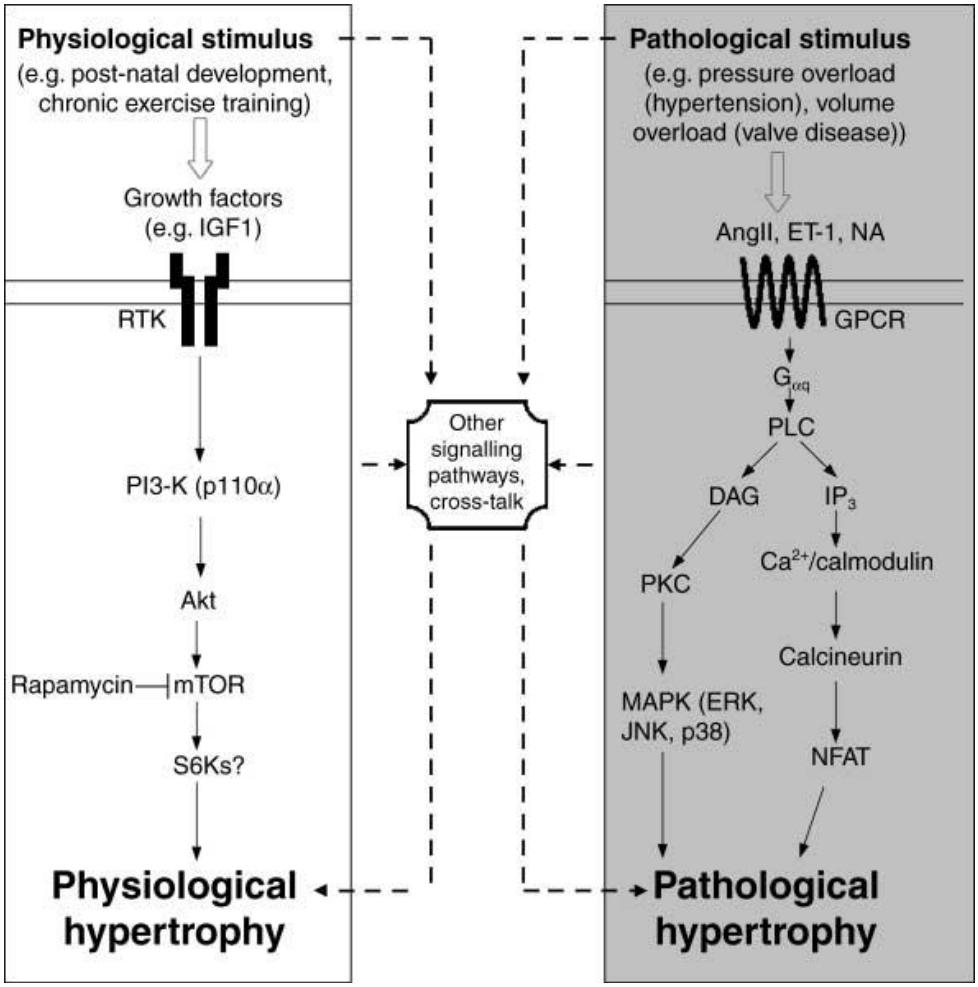

Figure 3: Signaling events in physiological and pathological cardiac hypertrophy. Depending on the stimulus, different signaling pathways may be involved in cardiac hypertrophy. The left panel roughly illustrates the signaling factors implicated as a result of physiological stimulus; the right panel illustrates signaling events occurring in response to pathological stimulus. (Reprinted by permission from John Wiley and Sons: Clin Exp Pharmacol Physiol 34(4):255-262, 2007).

inositol-triphosphate (IP3) and leads to the eventual activation of mitogen activate protein kinase (MAPK) and nuclear factor of activated T lymphocytes (NFAT), respectively (Frey and Olson, 2003; McMullen and Jennings, 2007).

As a result, the signaling pathways involved in pathological hypertrophy are extremely complex. A key player implicated in the activation of many of the intracellular pathways is calcium. The contraction cycle of the cardiomyocyte population is tightly regulated and coordinated in such a way that the beating cells can properly pump blood into and out of the respective chambers. The term used to describe this process is excitation-contraction coupling (ECC), and as in skeletal muscle, Ca^{2+} acts as the primary chemical gradient in this process. As such, fluctuations in intercellular calcium concentrations may provide a strong signal conduit to influence the development of cardiac abnormalities, including cardiac hypertrophy. Depending on the amplitude and duration of Ca^{2+} signaling, a variety of downstream effectors may be activated. The phosphatase calcineurin is activated in response to a sustained modest increase in $[Ca^{2+}]$ as opposed to a short spike in Ca^{2+} levels (Dolmetsch *et al*., 1997). The primary target of calcineurin is NFAT (Sugden, 1999; Molkentin, *et al*., 1998). NFAT becomes dephosphorylated by calcineurin which reveals a nuclear localization signal, and upon translocation to the nucleus, NFAT interacts with GATA4 to induce the upregulation of BNP (Molkentin *et al*., 1998). Crosstalk between calcineurin and MAPK signaling influences the overall activity of NFAT; MEK1 has been shown to enhance NFAT activity through ERK2 which is activated through the MAPK pathway following binding of α-adrenergic agonists, indicating

a convergence of signals initiated from intracellular calcium levels, and extracellular signaling through GPCRs (Sanna *et al*., 2005). However, signaling control of NFAT is very complex as other phosphorylation events, including those mediated by the p38 and JNK MAPKs, appear to directly inhibit NFAT activity by phosphorylation and subsequent inhibition of nuclear translocation (Braz *et al*., 2003; Sanna *et al*., 2005).

Despite the central importance of NFAT in mediating calcium dependent hypertrophic signals, this protein acts in conjunction with additional transcription factors, including GATA, MEF2 and Nkx2.5, to control the expression of numerous hypertrophy sensitive genes. Members of the MEF2 family of MADS box transcription factors are notable in this regard as they act as a point at which many hypertrophic signals converge. The transcriptional activity of MEF2 can be initiated by not only NFAT, but also CaMK, protein kinase D, calcineurin and MAPK (Barry and Townsend, 2010; Kim *et al*., 2008). Based on its role in hypertrophic regulation, MEF2 has an additional level of regulation in which it is suppressed by the binding of Class II histone deacetylases (HDACs). This inhibition can be relieved through HDAC phosphorylation, which triggers its nuclear export and allows for the transcription of MEF2 target genes (Fielitz *et al*., 2008).

Understanding the signaling mechanisms which underlie the hypertrophic response is imperative to elucidating future therapeutic targets. It is interesting to note that the transition from cardiac hypertrophy to heart failure (HF) has been

shown to involve few of the same signaling factors responsible for signaling during hypertrophy. For example, calcium, as described earlier, is involved in many aspects of hypertrophic signaling; however calcium dyshomeostasis is now widely accepted as contributing to the transition from hypertrophy to HF (Barry and Townsend, 2010). A key characteristic of HF is the increase of apoptosis and subsequent loss of cardiomyocytes (Jiang *et al*., 2003). Therefore, it may be a reasonable supposition that the key regulatory factors that mediate apoptosis may also act to influence the initiation and/or progression of cardiomyocyte hypertrophy. Indeed, key cell death proteins such as the caspase protease family have been shown to directly influence numerous cellular events independent of apoptosis, including differentiation, proliferation and the adaptive immune response. What is interesting to note, and what will be a major focus of the upcoming sections, is that caspase proteases have been shown to interact with many of the key regulators of the hypertrophic process. Therefore, a caspase protease may act to mediate the hypertrophic process and may indeed pre-empt the transition to HF.

1.3 Caspase Proteins and Apoptosis

Caspases are a family of proteolytic enzymes which have been primarily described in a cascade of signaling events leading to apoptosis, appropriately deemed the caspase cascade. Fourteen mammalian caspases have been described to date and they can be further classified as initiator or effector caspases depending on their role within the cascade. These proteins possess a cysteine residue within their active site and recognize consensus sequences

typically containing four amino acids, where they then hydrolyze the peptide bond on the carboxyl end of an aspartic acid residue, thereby classifying caspases as cysteine aspartases (Earnshaw *et al*., 1999; Timmer and Salyesen, 2007). Caspases are generally inactive within the cell, as zymogens that must be cleavage activated in order to activate subsequent downstream caspases. Two separate cleavage events are required to activate these enzymes; the first step is to free the N-terminal subunit from the catalytic subunit, and the second step is to cleave the two subunits (Earnshaw *et al*., 1999).

The caspase cascade may be initiated through two primary mechanisms, typically referred to as intrinsic or extrinsic stimuli. Extrinsic signals such as Fas Ligand may be received through a death receptor such as Fas, of the tumor necrosis factor (TNF) family of receptors. These receptors contain associated death domains within their cytoplasmic tails (Aggarwal, 2003; Hudek *et al*., 2007). The signal from FasL may be transduced into the cell through an adaptor protein, Fas Associated Death Domain (FADD), which also serves to recruit the initiator caspase, caspase-8 through interaction with a Death Effector Domain (DED). Once recruited to the receptor, caspase-8 may become activated through autocatalysis, which allows for the further transduction of the signal towards the nucleus as caspase-8 is able to cleave and activate caspase-3, an effector caspase, initiating a cascade of proteolytic events that compromise cell integrity (Aggarwal, 2003). Death signals may also arise from within the cell itself, using what is referred to as the intrinsic apoptotic pathway. Here, cytochrome C is released from the mitochondria in times of stress and can bind

with apoptosis activating factor-1 (Apaf-1) to recruit and activate pro-caspase-9, to produce the apoptosome (Hengartner, 2000). Once activated, caspase-9, another initiator caspase, can cleave and activate caspase-7, which can then activate caspase-3 as illustrated in Figure 4.

The activation of caspase-3, either by intrinsic or extrinsic signaling, causes subsequent cleavage of proteins that are vital to the cell's integrity, including lamin A and actin (Fischer *et al*., 2003). Eventually, caspase-3 cleaves inhibitor of caspase-activated DNase (ICAD) and subsequently releases CAD, which may translocate into the nucleus and cause the characteristic degradation of DNA into nucleosome sized fragments, completing the dissolution of the cell (Cory, 1998; McIlroy *et al*., 1999). Additional morphological characteristics of apoptosis include cell shrinkage, membrane blebbing, the formation of and the formation of apoptotic bodies (Hengartner, 2005; Kamada *et al*., 2005).

Although the apoptotic function of caspases has been described thus far, caspases may be involved with either cellular apoptosis, or cytokine maturation (Stennicke and Salvesen, 1999). Classically apoptotic caspases can be further identified as either initiator or effector caspases, depending on their role and substrates within the cell. Initiator caspases consist of caspases -2, -8, -9, and -10, and executioner caspases include caspases-3, -6, and -7. The roles for initiator and effector caspases have been discussed earlier, however, with respect to cytokine maturation, caspase-1 and caspase-11 have emerged as key

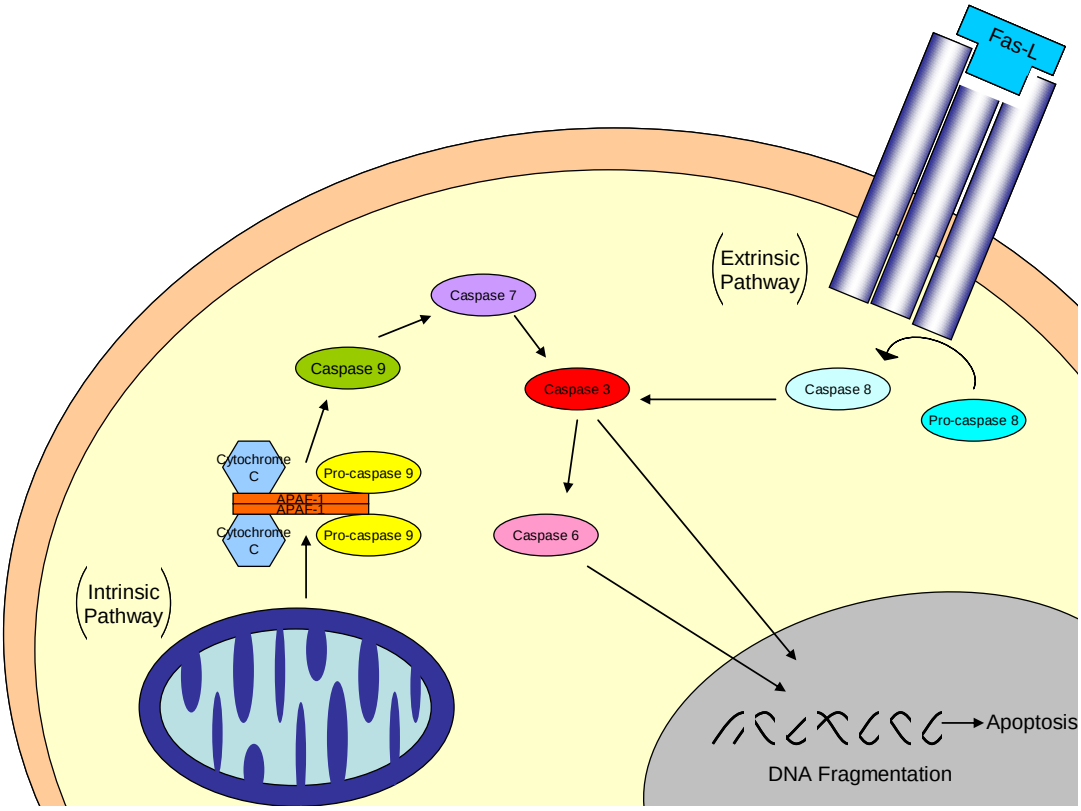

Figure 4: Apoptotic signaling; caspase cascade. Release of cytochrome c from the mitochondria can lead to the activation of initiator caspase, caspase-9. Binding of Fas ligand (Fas-L) can lead to the activation of initiator caspase, caspase-8. Once activated, initiator caspases can cleave and activate effector caspases including caspase-3 which leads to the apoptotic phenotype including DNA fragmentation.

regulators. To this end, caspase-11 has been implicated in the activation of caspase-1, which in turn is responsible for the processing of mature Inter-Leukin-1_{β}, (IL-1_{β}) (Kang *et al*., 2002). Caspase-11 has additional non-apoptotic effects within splenocytes and peritoneal macrophages whereby a null mutation is responsible for migration defects and disruption of cytoskeletal and actin dynamics (Li *et al*., 2007). There is some redundancy between several caspases and their respective roles and substrates; human caspase-4 and caspase-5 are thought to be orthologs of mouse caspase-11, although no conclusive substrates have been identified (Martinon and Tschopp, 2007). Caspase-12 has been thought to be involved in endoplasmic reticulum (ER) stress response, however this theory is quite controversial and has encountered much scrutiny (Martinon and Tschopp, 2007; Obeng and Boise, 2005). With respect to substrate redundancy, most caspase members have demonstrated the ability to cleave sequences containing DEVD *in vitro*, however PARP, a substrate with a cleavage site of DEVD is cleaved much more efficiently by caspase-3 and caspase-7 than any other caspase *in vivo* (Puig *et al*., 2001). In contrast, another key executioner caspase, caspase-6 has exclusive specificity towards VEID, with a unique preference for valine in the recognition sequence (Talanian *et al*., 1997). Due to the fact that some redundancy does exist between targeted caspase sequences, it is sometimes difficult to exclusively inhibit a single caspase. Despite this limitation, many of the enzymatic mechanisms involved in caspase cleavage and inhibition have been elucidated through studies using specific caspase inhibitors.

1.4 Non-apoptotic roles and specificities for members of the caspase family

The homeostatic balance between cellular proliferation, differentiation, and apoptosis is critical to the maintenance of health and viability in the multi-cellular organism. Caspases have classically been known for their contribution to the apoptotic aspect of this balance. Recently however, evidence has been found to support the theory that caspases may not only control apoptosis within an organism, but that they may in fact act as regulators for key cell fate decisions (Fernando and Megeney, 2007; Milligan and Schwartz, 1997). It has been suggested that caspases may act in either an apoptotic or non-apoptotic fashion, depending on the timing and amplitude of the stimulus (Fernando and Megeney, 2007). There are several convincing examples of studies that have shown caspase activation does not result in cell death (Okuyama *et al*., 2004; Fernando *et al*., 2002; Riento and Ridley, 2003; Abdul-Ghani *et al*., 2011).

Transgenic mouse models may provide the most convincing argument for caspases being responsible for more than simply cell death within an organism. The caspase-$3^{-/-}$ mutant mouse is notably smaller than wildtype littermates due to impairments in skeletal muscle differentiation (Fernando *et al*, 2002); and the caspase-$8^{-/-}$ mutation is embryonic lethal with observed impairment in heart muscle development and extensive cardiomyocyte apoptosis which may be explained by a requirement of caspase-8 for angiogenesis in the yolk sac (Varfolomeev *et al*., 1998; Sakamaki *et al*., 2002). At a cellular level, many characteristics exhibited during apoptosis are also observed during non-apoptotic

cellular events. For example, cytoskeletal reorganization has been demonstrated during terminal differentiation of epithelial cells (Derynck and Akhurst, 2007); the process of spermatogenesis involves cytoplasmic changes reminiscent of apoptosis; as well, the exclusion of the cells' nuclei occurs during erythropoiesis (Carlile *et al*., 2004). Furthermore, caspase-induced breaks in DNA, which have been widely considered to be indicative of apoptosis, have recently emerged as being required for skeletal muscle differentiation (Larsen *et* al., 2010). Here, the caspase-3 substrate, CAD, has been implicated in the formation of strand breaks seen during differentiation, such that inhibition of either CAD or caspase-3 was able to block the strand breaks and subsequent skeletal muscle differentiation.

Additional examples of non-apoptotic roles for caspases can be found in B lymphocyte progenitors and immune cell development, as well as differentiation of the myeloid lineage and T cell proliferation (Kang *et al*., 2004; Salmena *et al*., 2003; Schwerk and Schulze-Osthoff, 2003). Of particular relevance is the demonstration that caspase-3 is involved in the differentiation of cardiomyocytes, hypothesized to be mediated through signaling of a G protein coupled receptor (GPCR), Frizzled, and shown to suppress the canonical Wnt/β-catenin pathway (Abdul-Ghani *et al*., 2011). Through the course of cardiac differentiation, wingless (Wnt) proteins have emerged as essential factors (Pandur *et al*., 2002). Following the observation that caspase activity was increased during cardiac differentiation, a substrate was identified in β-catenin, and it was demonstrated that caspase-3 mediated cleavage of this protein was effective in blocking cardiac differentiation (Abdul-Ghani *et al*., 2011). In the context of the present

study, these findings support the notion that caspases may be active in the hypertrophic response within cardiomyocytes as the signal from PE is transduced through α-Adrenergic GPCRs, and furthermore the molecular principles governing cardiac hypertrophy have been clearly shown to emulate those of differentiating cardiomyocytes.

1.5 A Potential Requirement for Caspases during Cardiac Hypertrophy

In addition to these previously described non-apoptotic roles for caspases, these proteases have also been implicated in cardiac specific events, including several of the signaling mechanisms active during cardiac hypertrophy. One study in particular suggested a requirement for caspase-3 in pathological but not physiological hypertrophy in rats (Balakumar and Singh, 2006). To this end, chemical inhibition of caspase-3 abrogated cardiac hypertrophy and left ventricular dysfunction induced by partial abdominal aortic constriction (PAAC). In contrast, this study found that chemical inhibition of caspase-3 did not affect the physiological response induced by chronic swim training. What remained to be elucidated was whether this effect of caspase inhibition was cell autonomous.

Additional studies on the pharmacologic inhibition of caspases following MI have reported that reducing caspase activity limited the extent of left ventricular cardiac remodeling (Yarbrough *et al*., 2003; Yarbrough *et al*., 2010). Furthermore, myocyte-specific activation of caspases has been linked to changes in the contractile elements of the cell without showing signs of apoptosis

(Communal, *et al*., 2002). More recent investigations have found that inhibition of caspase activity following MI resulted in a corresponding reduction in the ratio of LV-weight-to-body-weight, less collagen deposition, decreased LV remodeling, and more preserved heart function (Chandrashekhar, *et al*., 2004).

Transgenic mice overexpressing cardiac-restricted TNF have also been shown to develop concentric cardiac hypertrophy, later leading to cardiac dilation and heart failure (Haudek et al., 2007). This study focused primarily on a cardioprotective role for Bcl-2 during sustained inflammation; however it was also found that apoptosis did not occur directly as a result of death signaling activation, suggesting that the downstream effectors of this signaling pathway may have been active in the hypertrophic process in the absence of cell death. Indeed TNF is a well-known activating ligand for extrinsic cell death signaling (see section 1.3). Another interesting mutant, the *Lpr* mouse, contains a point mutation that prevents normal Fas receptor signaling and also exhibits a blunted response to hypertrophic stimulus (Badorff *et al*., 2002). Despite these observations, a contributing or causative role for caspase activity in these models has not been explored.

Clearly, evidence is emerging to suggest that caspase proteases may impact the hypertrophy process. What remains unclear is whether caspases directly impinge on cardiomyocyte growth in a cell autonomous manner, or whether caspase activity indirectly influences hypertrophy. Elucidating a precise mechanism of action and substrate for caspases in the hypertrophic process will

be a priority. Indeed, several possibilities exist as to how caspases may act within the cardiomyocyte to influence this growth. For example, class II HDACs interact with MEF2 within the nucleus to suppress the transcription of MEF2 target genes. Upon phosphorylation, HDACs dissociate from MEF2 and exit the nucleus, relieving MEF2 suppression and allowing the transcription of downstream target genes, including those of the fetal gene program (Zhang *et al*., 2002). Notably, while HDACs are typically regulated through phosphorylation events controlled by calcium-calmodulin dependent kinases (CaMKs) or protein kinase D, both HDAC-4 and HDAC-7 have conserved caspase cleavage sites and have been shown to be cleaved by caspase-3 and caspase-8, respectively (Fielitz *et al*., 2008; McKinsey *et al*., 2000). Furthermore, HDAC-7 has emerged as the most readily cleaved caspase-8 substrate described thus far, and its cleavage is also associated with an abrogation of its repressor abilities, thus providing an example of caspase mediated regulation of transcription (Scott *et al*., 2008). As such, it is reasonable to postulate that the interaction between HDAC-4, which contains a caspase-3 cleavage site, and MEF2 could be negated by caspase cleavage, to similarly relieve MEF2 repression and allow the subsequent transcription of hypertrophic target genes.

Alternatively, it is possible that caspases could exercise their role in hypertrophy through calcineurin signaling. The role for calcineurin in cardiac hypertrophy has been very well characterized as being activated upon increases in calcium concentration and by cleavage with calpain (Barry and Townsend, 2010; Huang *et al*., 2010); however calcineurin activation via cleavage by

caspase-3 has not been investigated in this context. Indeed, calcineurin has been shown to be cleaved by caspase-3 in cases of glaucoma, and during NFAT dependent expression of IL-2 in Jurkat T-cells (Huang *et al*., 2010; Mukerjee *et al*., 2001). It is therefore conceivable that calcineurin may be similarly regulated by caspases during cardiac hypertrophy.

1.6 Objective and Hypothesis

Although several studies have investigated non-apoptotic roles for caspase proteases in cardiac adaptation, these studies have primarily focused on using *in vivo* models, and have not addressed many of the underlying questions as to how caspases may influence this biological process at the cellular level. It is generally accepted that caspases play an integral part in many of the signaling pathways required for normal cellular maintenance, proliferation, and differentiation; and there are several examples in the literature where caspases have also been implicated in cardiac hypertrophy. Therefore, this study intends to determine the role (if any) of caspase proteases as a cell autonomous signal that promotes hypertrophy of the cardiomyocyte.

Objectives

Using primary neonatal rat ventricular cardiomyocytes, determine

a) the effect of caspase-3 and caspase-8 inhibition on cardiomyocyte morphology when induced to undergo hypertrophy

b) the amount of caspase-3 and caspase-8 activity present in cardiomyocytes undergoing hypertrophy

c) if there is a change in subcellular localization of caspase-3 and/or caspase-8 in response to hypertrophic induction

Hypothesis

Caspase-3 and/or caspase-8 are required for cardiac hypertrophy to occur *in vitro*, either as a result of increased activity or a change in cellular localization.

CHAPTER 2

Materials and Methods

2.1 The Isolation and Respective Treatments of Primary Cardiomyocytes

The hearts of 10-30, 1-4 day old Sprague-Dawley rats (Charles River Canada, Montreal, QC) were excised and placed in Joklik's Modified Eagles Medium (J-MEM) (1.13 g Minimum Essential Medium Joklik's, SAFC Biosciences, Lenexa KS, 0.2 g Sodium Bicarbonate, in 100 mL dH_2O) at room temperature until all hearts had been collected. The atrial tissue was separated from the ventricles, and the following digestion was performed on both tissues in separate dishes and tubes, simultaneously. The tissues were minced into pieces approximately 1 mm^3 in size and transferred to a Falcon tube containing 220 U/mL Collagenase II (Collagenase Type II, Worthington Biochemical Corporation, Lakewood NJ) in Joklik's-MEM for five rounds of digestions of 15 minutes each at 37°C with agitation. When more than 12 hearts were being digested, the tissue was split into two digestion tubes to normalize the collagenase to tissue ratio. After discarding the first supernatant, 5 cellular fractions were collected and the supernatants were transferred to tubes containing 5 mL of FBS (Invitrogen, Grand Island NY) to prevent further digestion and centrifuged at 100xg for 5 minutes. Cell pellets were then resuspended in DMEM culture media (10% FBS,100 U/mL Penicillin/100 µg/mL Streptomycin, Invitrogen, Grand Island NY, in Dulbecco's Modified Eagle Medium (DMEM), Invitrogen, Grand Island NY). Following completion of enzymatic digestion, the ventricular and atrial cell pellets were each pooled and filtered through 74 µm Netwell filters (Corning Life Science, MA). Cell suspensions were then subject to

two rounds of 30 minute pre-plating on Petri dishes at 37°C and 5% CO_2. The resulting cardiomyocyte enriched culture was then collected using centrifugation at 100xg for 5 minutes; cells were resuspended and counted using a haemocytometer, and plated either onto 35 mm collagen-coated dishes (Roche, Mannheim Germany; prepared in 0.02% acetic acid to a final concentration of 2 mg/mL) at concentrations of 5.0×10^5 cell/mL for caspase assays and RNA isolation, or onto collagen coated coverslips at a concentration of 2.5×10^5 cells/mL for immunocytochemistry. Cells were allowed to recover for a period of 16-20 hours in DMEM culture media. Following this incubation, the media was changed to serum-free (SF) media (1 g BSA Fatty Acid free, low endotoxin, Millipore Corporation, Kankakee IL, 50 mL DMEM, 0.53 g Cellgro Ham's F-12 Medium (Modified), Mediatech, Inc. Herndon VA, 0.3 g HEPES, Invitrogen, Grand Island NY, 2 mL Penicillin/Streptomycin, 100 µL Apo-Transferrin, Sigma, St. Louis MO, 100 µL ITS Culture Supplement, Sigma, St. Louis MO, 40 µL Calcium Chloride dehydrate, in dH_2O) for 24 hours before treatments were initiated. Wherever indicated, caspase inhibitors Z-DEVD-FMK and Z-IETD-FMK (BioVision, Mountain View CA) were used at a concentration of 20 µM and pre-treated for 2 hours before hypertrophic agonists were added. Phenylephrine (PE), (Sigma, St. Louis MO) was used at a concentration of 100 µM in SF media, and FBS was used at 10% for the induction of hypertrophy. Media was refreshed every 24 hours and maintained at 37˚C with 5% CO_2 for the times indicated in the respective experiments, ranging from 3 hours to 72 hours.

2.2 Protein Isolation and Quantification

Protein was isolated from cells grown on 35 mm plates as follows. Cells were gently washed with phosphate buffered saline (PBS), pH 7.4 (137 mM NaCl, 2.7 mM KCl, 10 mM Na_2HPO_4, 1.8 mM KH_2PO_4) scraped into 1.5 mL eppendorf tubes and centrifuged at 3700 rpm for 5 minutes at 4˚C. 200 µL of caspase lysis buffer (1 M Tris-HCl pH 7.5, 5% NP-40, 5% Na-Deoxycholate, 5 M NacCl, 0.2 M EGTA) was added to the pellets which were then incubated at 4˚C for 1 hour on a rotator. Samples were centrifuged at 13000 rpm for 10 minutes at 4˚C and supernatants retained for protein quantification. Concentrations were determined using Bradford assay (Biorad, ON) and UV spectrophotometry at 595 nm using an Ultrospec 2100 pro UV/Vis Spectrophotometer.

2.3 Caspase Activity Assays

20 µg protein was loaded into individual wells of a 96-well dish containing a combined volume of 198 µL with the addition of caspase activity buffer (5 M HEPES-NaOH pH 7.5, 25% Sucrose (w/v), 5 M EDTA, 5% CHAPS, 1 M DTT). 100 µM caspase-3 or caspase-8 substrate, Ac-DEVD-AMC or Ac-IETD-AMC (Enzo Life Sciences, Plymouth Meeting, PA) was added to each well and fluorescence was measured at an excitation wavelength of 380 nm and emission wavelength of 460 nm for 6 hours using a Fluoroskan Ascent Fl (ThermoLabsystems). Results were obtained using Ascent Software and analyzed using Microsoft Excel. These values from the linear fluorescence progression was used for comparison of overall caspase activity, which was

normalized to caspase activity buffer only controls, and further normalized to caspase activity at time-0 across individual trials.

2.4 RNA Extraction and Reverse-Transcriptase PCR (RT-PCR)

RNA was collected from cells grown on 35 mm collagen coated plates. Cells were washed in PBS before 750 µL of TRIzol reagent (Invitrogen, CA) was added to each sample and incubated for 5 minutes at room temperature with gentle swirling. Cells were then scraped and collected in RNase-free 1.5 mL eppendorf tubes and incubated at room temperature for 5 minutes. 150µL chloroform (Fisher Scientific, Ottawa ON) was added to each tube which was then vortexed and incubated at room temperature for 3 minutes. Tubes were centrifuged at 10 000xg for 10 minutes at 4˚C and supernatants were transferred to new RNase-free eppendorf tubes. 450 µL iso-propanol was added to each sample, and samples were mixed gently at room temperature for 20 minutes before being centrifuged at 10 000xg for 15 minutes at 4˚C. Pellets were washed with 500 µL 70% EtOH-DEPC and then centrifuged for an additional 5 minutes at 7500xg at 4˚C. Pellets were air dried and resuspended in 30 µL H_2O-DEPC then incubated at 4˚C for 1 hour before being transferred to -20˚C for storage.

RNA was quantified using an Ultrospec 2100 pro, and 2 µg RNA was used for synthesis of complementary DNA (cDNA) using RT-PCR. Briefly, RNA samples were incubated with 1 µL 500µg/mL (Primer) Oligo (dT15) (Invitrogen, Carlsbad CA) and 1 µL dNTP Mix (Roche Diagnostics, Mannheim Germany) at 65°C for 5 minutes, followed by the addition of 4 µL 5X 1st strand buffer

(Invitrogen, Carlsbad CA), 2 µL 0.1M DTT (Invitrogen, Canada) and 1 µL RNase Inhibitor (2000 units) (Roche Diagnostics, Indianapolis IN) with incubation at 42°C for 2 minutes. 1 µL Superscript II (Invitrogen, Carlsbad CA) was then added to samples which were incubated at 42°C for 50 minutes. Samples were heat inactivated at 72°C for 15 minutes and lastly 1 µL RNase H (Invitrogen, Carlsbad, CA) was added before incubation at 37°C for 20 minutes. cDNA samples were stored at -20°C.

2.5 Real-Time Polymerase Chain Reaction

cDNA was diluted in water to a 1:5 dilution for qPCR analysis. 200 ng of cDNA was added to 10 µL Quantifast SYBR green PCR reaction mix (Qiagen, Mississauga, ON) and 4 µL 5µM forward and reverse primers (Alpha DNA) as described in Table 1. Reactions were performed using an Mx Pro-Mx3000P Thermocycler and RotogeneQ according to the manufacturer's instructions. A thermal profile of 5 minutes initial denaturation at 95˚C, 40 cycles of 10 seconds denaturation at 95˚C, 30 seconds annealing at 60˚C, and 30 second extension at 72˚C was followed. Final elongation was carried out at 72˚C for 5 minutes. All cDNA samples were analyzed in duplicate and normalized to GAPDH expression. Results were compiled using Excel (Microsoft). Primers listed below were designed using Primer3 (Massachusetts Institute of Technology) software.

Table 1: Primers used for Real-Time PCR

Gene	Primer Sequences
ANF	L: 5'-CTGCTAGACCACCTGGAGGA-3' R: 5'-AAGCTGTTGCAGCCTAGTCC-3'
GAPDH	L: 5'-GGCATTGCTCTCAATGACAA-3' R: 5'-TGTGAGGGAGATGCTCAGTG-3'

2.6 Immunocytochemistry

Cells grown on collagen coated coverslips for immunocytochemistry were washed with 1X PBS twice and were fixed using 4% paraformaldehyde (PFA) (Fisher Scientific, Ottawa ON) for 10 minutes. 1% Bovine serum albumin (BSA) (Roche Diagnostics, Mannheim Germany) was used for blocking with 0.3% Triton-X (Sigma-Aldrich) for permeabilization. Cardiomyocytes were stained with α-actinin at a dilution of 1:800. Active caspase-3 was stained with 1:200 α-active caspase-3 (BioVision, Mountain View CA) and active caspase-8 was stained with 2 µg/mL α-active caspase-8 (Abcam, Cambridge, MA). Secondary antibodies AP192Flour and Cy3 were used at concentrations of 1:200 (Chemicon, Temecula CA). Nuclei were stained with 1:10000 4',6-diamidino-2-phenylindole (DAPI) in H_2O, as described in Table 2. Coverslips were mounted on slides using DAKO mounting media (Dako Cytomation, Denmark). Cells were imaged on either an inverted microscope, Zeiss Observer Z.1 using the AxioCam HRm camera and obtained using AxioVision software, or on a confocal microscope, Confocal- LSM 510 Meta (Zeiss), using AxioVision software. Images were further analyzed using ImageJ software.

Table 2: Antibodies used for immunocytochemistry

Antibody	Supplier	Animal Origin	Working Concentration
Anti-α-Actinin	SigmaAldrich	Mouse	1:800
Anti-Caspase-3 (Active)	BioVision	Rabbit	1:100
Anti-Caspase-8 (Active)	Abcam	Rabbit	2µg/mL
Anti-Mouse, AP192Fluor	Chemicon	Donkey	1:200
Anti-Mouse, Cy3 AP124C	Chemicon	Goat	1:200
Anti-Rabbit, Cy3 AP182C	Chemicon	Donkey	1:200
Anti-Mouse, Alexa-594	Invitrogen	Goat	1:1000
Anti-Mouse, Alexa-488	Invitrogen	Goat	1:1000

2.7 Recombinant Adenovirus Production and Viral Infection

Baculovirus *Californica autographica* encoding full-length p35 cDNA was provided by Dr. Kazuhiro Sakamaki (Institute for Virus Research, Koyoto University, Koyoto, Japan). The viral shuttle construct arrived as a DNA plasmid and a digestion was performed to isolate the p35 coding sequence, internal ribosome entry site, and eGFP from the plasmid using *EcoRI* and *NotI*; these genes were then sub-cloned into a pShuttle vector under the CMV promoter using blunt-end cloning. The fragment was then inserted into an adenoviral genome deficient in E5/E3 genes by linearizing PShuttleCMV_p35_IRES_eGFP and subsequently electroporating this into a RecA+ BJ5183 *Escherichia coli* containing the pAdeasy1 plasmid (Stratagege, La Jolla CA). The final adenoviral construct resulted from homologous recombination. Clones were selected and transformed into DH5α E. coli*;* a cesium chloride gradient ultracentrifugation was used to purify the DNA. The stock virus was generated through linearization of the plasmid encoding an E-1 recombinant adenoviral genome, using restriction

enzyme *PacI* followed by transfection into HEK293 cells using Lipofectamine 2000 (Invitrogen Life Technologies, Carlsbad CA). The virus was amplified further by additional infections of the HEK293 cells, and finally purified using cesium chloride banding. Titers were determined through measuring the absorbance at 260 nm.

Cells subject to adenoviral infection were isolated as described in section 2.1 and similarly allowed 24 hours in DMEM culture media to adhere to the collagen coated cover slips and recover from the isolation. After 24 hours, the virus was introduced to the cells at a multiplicity of infection (MOI) of 10.0, at the same time that serum-free media was introduced to the cells. 24 hours later, the media was either refreshed or changed to hypertrophic media containing 100 μM PE. Cells were fixed and stained as described in section 2.5, following 24 hours of the respective treatments.

2.8 Statistical Analysis

A minimum of three biological repeats were performed for each experiment. The results are presented as the average of each data set, and error bars are representative of standard error of the mean (S.E.M.). Tests for statistical significant were conducted using Students' T-tests or analysis of variance (ANOVA) where indicated. A P-value of less than 0.05 was used as the determinant for significance.

CHAPTER 3

Results

3.1 Simultaneous inhibition of caspase-3 and caspase-8 minimizes phenylephrine and FBS induced cardiac hypertrophy

Cardiac hypertrophy was induced in a neonatal rat ventricular cardiomyocyte cell model using 100 μM phenylephrine (PE) and 10% fetal bovine serum (FBS). Caspase-3 and caspase-8 were simultaneously inhibited using 20 μM chemical inhibitors Z-DEVD-FMK and Z-IETD-FMK. The effects of caspase inhibition on hypertrophic growth were monitored in part through immunocytochemistry as cells were stained for cardiac-specific α-actinin. Comparison of cardiomyocyte size was done through fluorescence microscopy using an inverted microscope and AxioVision and ImageJ software. Figure 5a summarizes the effects of caspase inhibition on PE and FBS induced hypertrophy. All indicated cell areas are reported relative to untreated cells at time-0.

The hypertrophic agonists were found to induce an increase in cell size of approximately 125% following 24 hours of treatment. This growth was increased to 350% after 72 hours of treatment. The addition of the pharmacological caspase inhibitors to hypertrophic media significantly reduced the hypertrophic effect of FBS and phenylephrine after 24 hours, as cardiomyocyte size increased by 30% which was not found to be significantly different than that of the serum-free treated cells ($P>0.05$) (Figure 5). Following 72 hours of treatment, caspase inhibition was found to reduce the hypertrophic response by approximately 50% ($P>0.05$, Figure 5). Although this trend continued throughout the time course

examined, some hypertrophic cells appeared to grow to a much greater extent than others at the later times. More specifically, some cardiomyocytes experienced an increase in cell area of up to a 400% upon hypertrophic induction, whereas other cardiomyocytes grew only a fraction of their initial size. The distribution of these cell sizes was analyzed and is included in Appendix I. While the average size of those cells treated with PE, FBS, caspase-3 and caspase-8 inhibitors was less than that in the uninhibited hypertrophic culture, as indicated in Figure 5a, Appendix I provides more information into the variability of the extent of hypertrophy occurring in response to FBS and PE, and caspase inhibition. The significance of hypertrophic reduction in response to caspase inhibition was lost after 48 hours, perhaps due to variability in the hypertrophic response with FBS in the media. As a result, the following experiments focused on the first 24 hours of hypertrophy and 100 μM PE alone was used as an agonist.

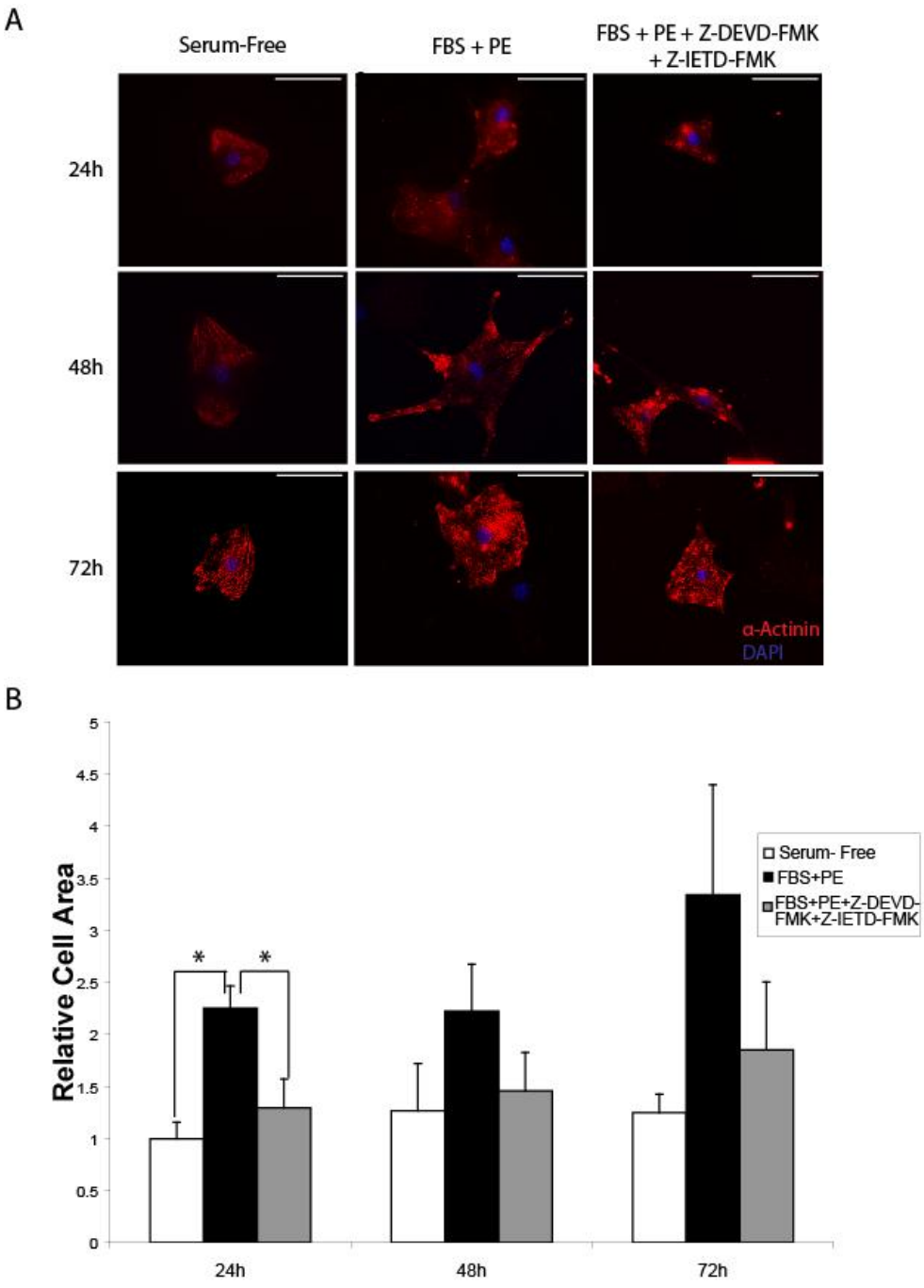

Figure 5: Effect of simultaneous caspase-3 and caspase-8 inhibition on PE and FBS induced hypertrophic growth. a) Neonatal rat ventricular cardiomyocytes were cultured over 72 hours in serum-free media (left panels), 100μM PE and 10% FBS (middle panels) and 100μM PE, 10% FBS, 20μM Z-DEVD-FMK and Z-IETD-FMK (right panels). Cardiomyocytes were stained with α-actinin (red) and DAPI (blue). b) Cell areas were measured using AxioVision and ImageJ software. Cells treated with serum-free media (white), 100 μM PE and 10% FBS (black), and PE, FBS, 20 μM Z-DEVD-FMK and Z-IETD-FMK were compared to untreated cardiomyocytes at time-0. *p<0.05 ANOVA; n=3.

3.2 Individual inhibition of Caspase-3 or Caspase-8 minimizes phenylephrine-induced hypertrophy in cardiomyocytes

Preliminary experiments suggested that caspase-3 and/or caspase-8 may be involved in the hypertrophic response in cardiomyocytes. Therefore further investigation into the effects of this inhibition was conducted using individual inhibition of the two proteases. The same commercially available pharmacological inhibitors, Z-DEVD-FMK and Z-IETD-FMK, were used at concentrations of 20 μM to inhibit caspase-3 and caspase-8, respectively. The morphological effects of the inhibitors, and 100 μM PE, on treated neonatal rat ventricular cardiomyocytes were monitored again using an antibody against α-actinin and fluorescent microscopy. Cell areas were measured using AxioVision and ImageJ software and were reported relative to vehicle-only treated cells maintained in serum-free media.

FBS was removed from the media in attempts to gain more insight into the potential pathways where caspases may be eliciting their effects. Because the mechanism in which PE induces hypertrophy has been well characterized, this approach aimed to limit potential substrates for future investigation. DMSO was added as an additional control for the vehicle in which the chemical caspase inhibitors were suspended. The effect of caspase inhibitors alone, without hypertrophic induction, was also examined and found to be negligible. Without FBS in the media, PE was found to induce an approximate 45% increase in cell size, which although not as great as that induced with FBS, was more consistent.

In cells receiving Z-DEVD-FMK in addition to PE, the hypertrophic growth was significantly reduced by over 60% ($P<0.05$, Figure 6c). Growth in those cells receiving Z-IETD-FMK in addition to PE was reduced by 51% relative to uninhibited PE treated cells; however this was not statistically different from either the SF or PE treated cells.

PE treatment was also associated with an enhancement in sarcomeric organization as indicated by the appearance of structured Z-disks throughout the cardiomyocytes (2nd panels of Figure 6a, b). Cytoskeletal reorganization is a hallmark of hypertrophy, and these cytoskeletal changes were monitored after 24 hours of the respective treatments. Cells were considered to possess sarcomeric organization when more than 50% of the cell exhibited structured sarcomeric units. PE treatment appeared to induce cytoskeletal reorganization in 70% of cardiomyocytes, which was significantly increased from 20% in DMSO treated cells. The addition of Z-DEVD-FMK significantly reduced the amount of PE-induced sarcomeric organization to 20% ($P<0.05$, Figure 6e), which was not statistically different than that of the vehicle-only control. Caspase-8 inhibition with Z-IETD-FMK also appeared to reduce the amount of sarcomeric organization, however, this was not found to be statistically significant. Inhibitor treatment alone was not found to significantly effect sarcomeric organization. In addition, the inhibitors did not appear to cause any significant changes in cardiomyocyte morphology, or size, in non-stimulated, serum-free conditions.

The effectiveness of the chemical caspase inhibitors was confirmed through caspase activity assays. Caspase-3 and caspase-8 were activated with 20 μM staurosporine (STS) (Appendix II Figure S. 2), with or without the inhibitors in culture. The vehicle for the inhibitors, DMSO, was not found to effect caspase activity on its own. Z-DEVD-FMK was found to decrease caspase-3 activity by 80%, and Z-IETD-FMK decreased caspase-8 activity by 55%.

3.2.1 The percentage of cardiomyocytes in culture does not appear to change in response to hypertrophy or caspase inhibition

The isolation protocol used in these experiments produced a heterogeneous cell population including, but not limited to, cardiomyocytes. To confirm the results shown in Figure 6 did not originate from a secondary effect from a non-cardiomyocyte population or by an alteration in cardiomyocyte cell survival, the percentage of cardiomyocytes, per total cell population, was determined for each of the respective treatment groups. Cardiomyocytes were stained with a cardiac specific marker and the number of α-actinin positive cells was compared to the number of total cells as measured by DAPI staining. As demonstrated in Figure 6d, the percentage of cardiomyocytes in culture did not appear to change in response to PE treatment, caspase-3, or caspase-8 inhibition. Cardiomyocytes were found to represent approximately 80% of the total cells present in the cell culture regardless of the treatment condition. As such, the alterations in cell size were determined to be cell autonomous and not a secondary effect of a changing cell population.

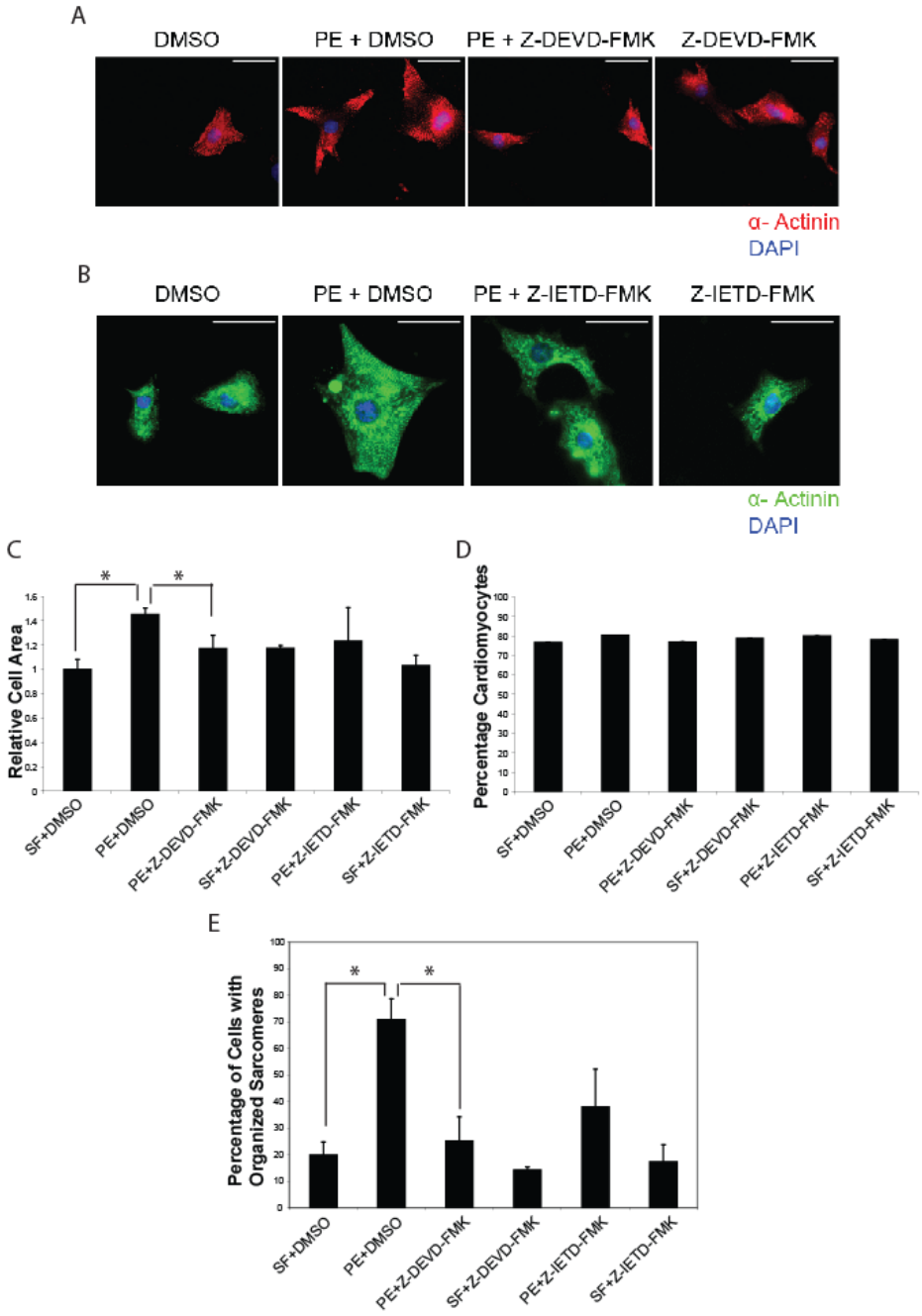

Figure 6: Effects of caspase-3 or caspase-8 inhibition on PE induced hypertrophic growth and sarcomeric organization. Cardiomyocytes were selectively stained and imaged as previously described. a-b) Cells were treated with DMSO as a vehicle-only control (1st panels); 100μM phenylephrine (2nd panels); 100μM phenylephrine and 20 μM Z-DEVD-FMK or Z-IETD-FMK, respectively (3rd panels); and the inhibitors alone (4th panels). c) Cell sizes were monitored using ImageJ and normalized to DMSO-only controls. d) The percentage of cardiomyocytes in culture was determined by comparison of α-Actinin positive cells to DAPI. e) The percentage of cardiomyocytes with at least 50% of structured sarcomeric units within the cell was monitored in response to the respective treatments; *P<0.05; n=3.

3.3 Molecular Inhibition of caspase activity using p35 prevented the increase in cell size associated with phenylephrine treatment

To eliminate the possibility that the chemical caspase inhibitors were having a non-specific effect that limited hypertrophy, the previous experiments were repeated using a broad spectrum molecular inhibitor of caspases, p35. This protein was delivered using a recombinant adenovirus encoding p35 at a multiplicity of infection (MOI) of 10.0. This MOI was determined following examination of infection efficiency using MOI's ranging from 0.1-100 through analysis of the GFP-tag under fluorescent microscopy (see Appendix III for calculation and infection efficiency).

Cells were isolated as described previously and as outlined in Figure 7a; the cells were infected with the p35 adenovirus (p35Ad) at the same time that serum-free media was introduced (-24hrs). Cells were allowed 24 hours for infection to occur and media was then changed to the respective treatments at 0hrs. Following 24 hours of 100μM phenylephrine treatment, uninfected cells experienced a 42% increase in cell size (Figure 7b, c, $P<0.05$). This increase in cell size was significantly diminished to 10% in those cells also infected with p35Ad ($P<0.05$). The virus alone was not found to significantly affect the size of cardiomyocytes ($P>0.05$). Based on these observations, p35 was found to limit the increase in cardiomyocyte size seen following 24 hours of phenylephrine treatment.

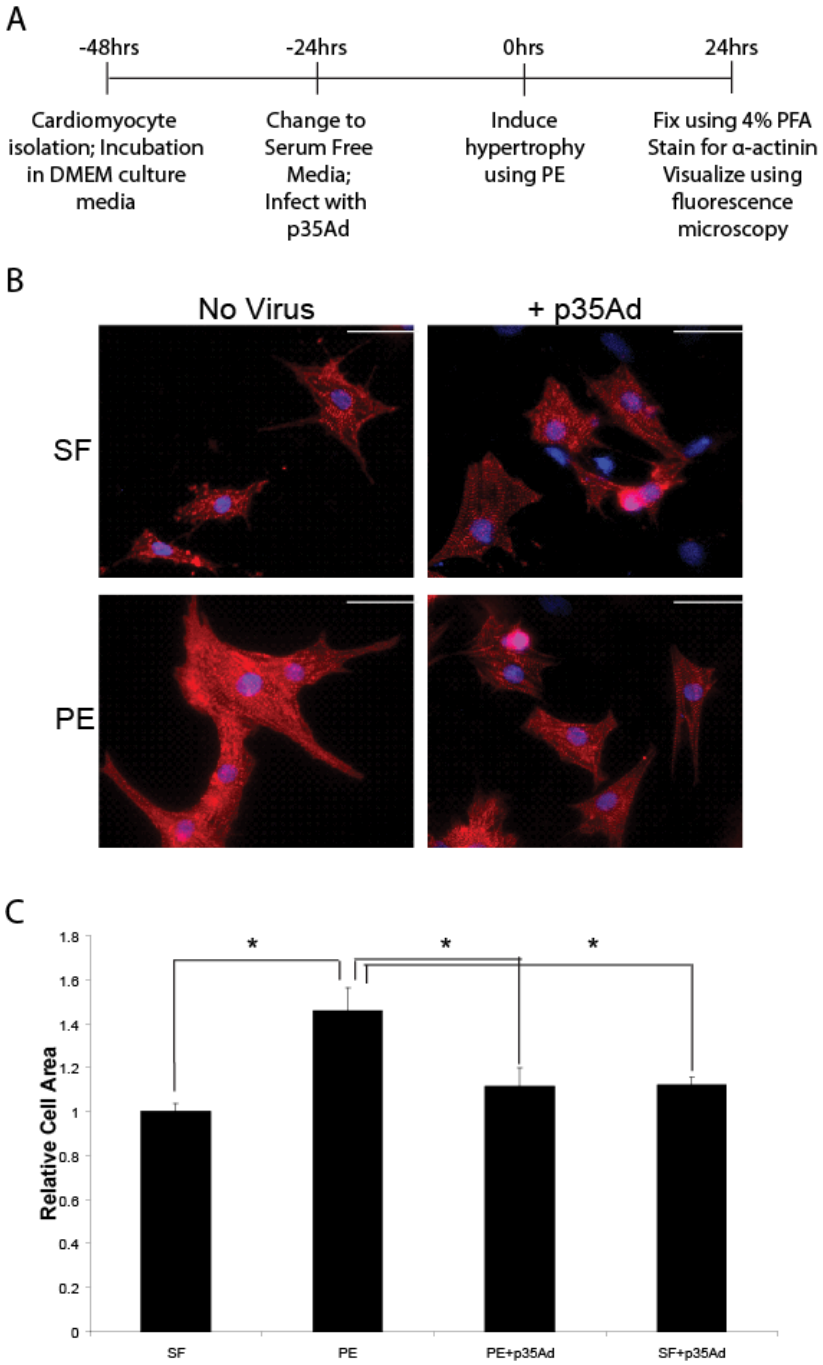

Figure 7: Effect of caspase inhibition through p35 on hypertrophic growth. a) Schematic for treatment of cardiomyocytes using molecular inhibition of caspases through p35Ad b) Cells were either infected with p35Ad or untreated; the two groups underwent treatment with SF or 100μM PE media. Cells were stained with α-actinin (red) and DAPI (blue) and analyzed using ImageJ; c) Cell area was measured relative to SF-treated cells, growth was deemed significant with a P-value of <0.05 using ANOVA; n=3.

The effects of the virus itself were examined through infection with a GFP containing adenovirus (GFP.Ad). Cardiomyocytes were infected at a range of MOI's, and again an MOI of 10 was used for optimal infection. 100 µM PE induced a 42% increase in the size of cardiomyocytes. With the addition of GFP.Ad to PE, this growth was increased to 49%. The presence of the GFP.Ad virus alone induced a 9% increase in cell size. The slight increase in cell area that may be associated with the presence of the virus mirrors what was observed with the addition of p35Ad. The significance of this result has yet to be determined through repetitions of the experiment; however, these findings suggest that the presence of the virus itself did not inhibit cell growth, and the reduction of hypertrophic growth was as a result of the presence of p35 and subsequent inhibition of caspases (Appendix III Figure S. 4).

Additionally, the effectiveness of p35Ad at inhibiting caspase activity was confirmed through the performance of caspase activity assays on p35 and GFP-only infected cells. P35 was found to completely eliminate caspase-3 activity, and decrease caspase-8 activity by over 80% as illustrated in Appendix II, Figure S. 2.

3.4 Global cellular caspase activity remained unchanged during in vitro cardiomyocyte hypertrophy

Typically, enhanced caspase function is associated with increased proteolytic activity rather than a simple protein interaction. Therefore, caspase activity was examined in cardiomyocytes at multiple time points throughout the first 24 hours of hypertrophy, and compared to the activity present in cells

maintained in serum-free media. Cells were collected and lysed using caspase lysis buffer following treatment in serum-free media, 100 μM PE and 10% FBS, or 100 μM PE alone for 3, 6, 12, or 24 hours as indicated in Figure 8. 20 μg of protein was added to a normalized volume of caspase activity buffer and incubated with caspase-3 or caspase-8 fluorometric substrate, Ac-DEVD-AMC or Ac-IETD-AMC, respectively, for 6 hours. Fluorescence was measured using a Fluoroskan Ascent Fl, as per the manufacturer's instructions. Activity increased in a linear manner over time and the maximum fluorescence reached was used in the following analysis. Caspase-3 and caspase-8 activity was first measured in cells treated with FBS and PE, and compared to that activity present in cells treated with serum-free media (Figure 8a, c). Protein was collected from cells following 6, 12, and 24 hours of the respective treatments. Caspase activity was normalized to that at time-0 across the three different trials. Cells receiving treatment with hypertrophic agonists appeared to have slightly less caspase activity than those treated in SF media; however this activity remained much less than that in the apoptotic, STS treated positive control, and the difference between caspase-3 and caspase-8 activity present in hypertrophic and serum-free treatments was not found to be statistically significant ($P>0.05$).

To address the possibility that FBS was contributing to the survival of the cardiomyocytes, and that some of the caspase activity was derived from an apoptotic response, FBS was removed from the culture media and caspase activity assays were repeated. A 3-hour time point was collected, in addition to the 6, 12, and 24 hour time points. Again, no significant difference in the total

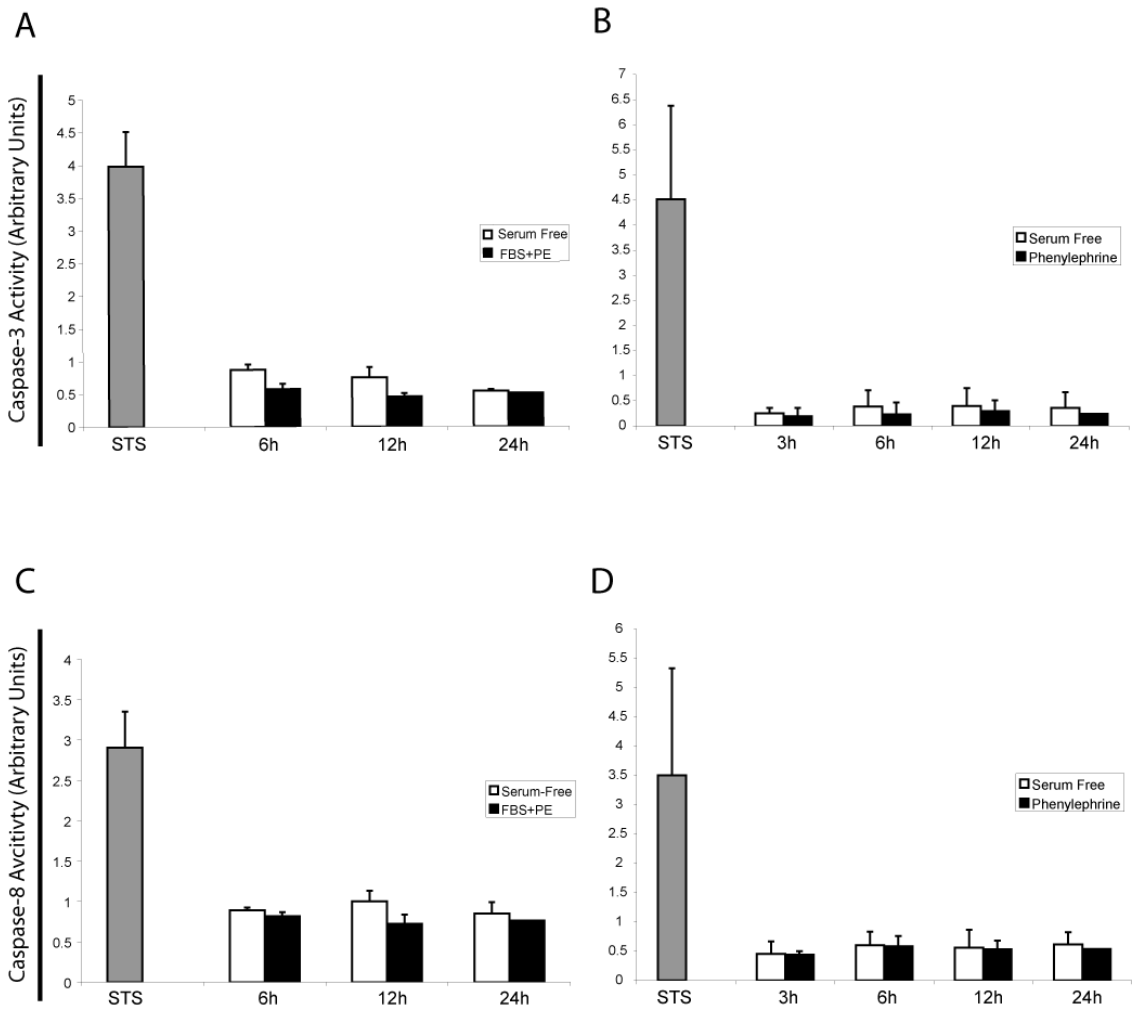

Figure 8: a-b) Caspase-3 activity was assessed using caspase activity assays with Ac-DEVD-AMC fluorogenic substrate throughout the first 24 hours of a) SF and FBS+PE treatment; and b) SF and PE treatment. c-d) Caspase-8 activity was assessed using caspase activity assays with Ac-IETD-AMC fluorogenic substrate throughout the first 24 hours of c) SF and FBS+PE treatment; and d) SF and PE treatment. Caspase activity has been normalized to T0 across trials; n=3.

amount of cellular caspase activity was observed between the phenylephrine and serum-free treated cells at these time points (Figure 8b, d).

3.5 Effects of caspase inhibition and phenylephrine treatment on ANF expression

Further investigation into the effects of caspase inhibition on the hypertrophic response was conducted through the study of ANF expression. ANF is a marker of cardiac hypertrophy and reflects the reversion to the fetal gene expression program (Lesniak *et al*., 1995). Here, ANF expression was measured quantitatively through real-time PCR.

Atrial tissue was used as a positive control for the expression of ANF. As noted in Figure 9, ANF expression increased roughly 3-fold in response to 24 hours of PE treatment, relative to DMSO treated controls ($P<0.05$). Both Z-DEVD-FMK and Z-IETD-FMK decreased the up-regulation of ANF by approximately 50% however this was not found to be statistically significant. The inhibitors alone appeared to cause a slight decrease in baseline ANF expression but this was not significantly different than DMSO treated cells. All experiments were conducted in duplicate and normalized to the expression level of house-keeping gene, GAPDH. (See Appendix IV for additional information regarding real-time PCR analysis and an example of the data processing.)

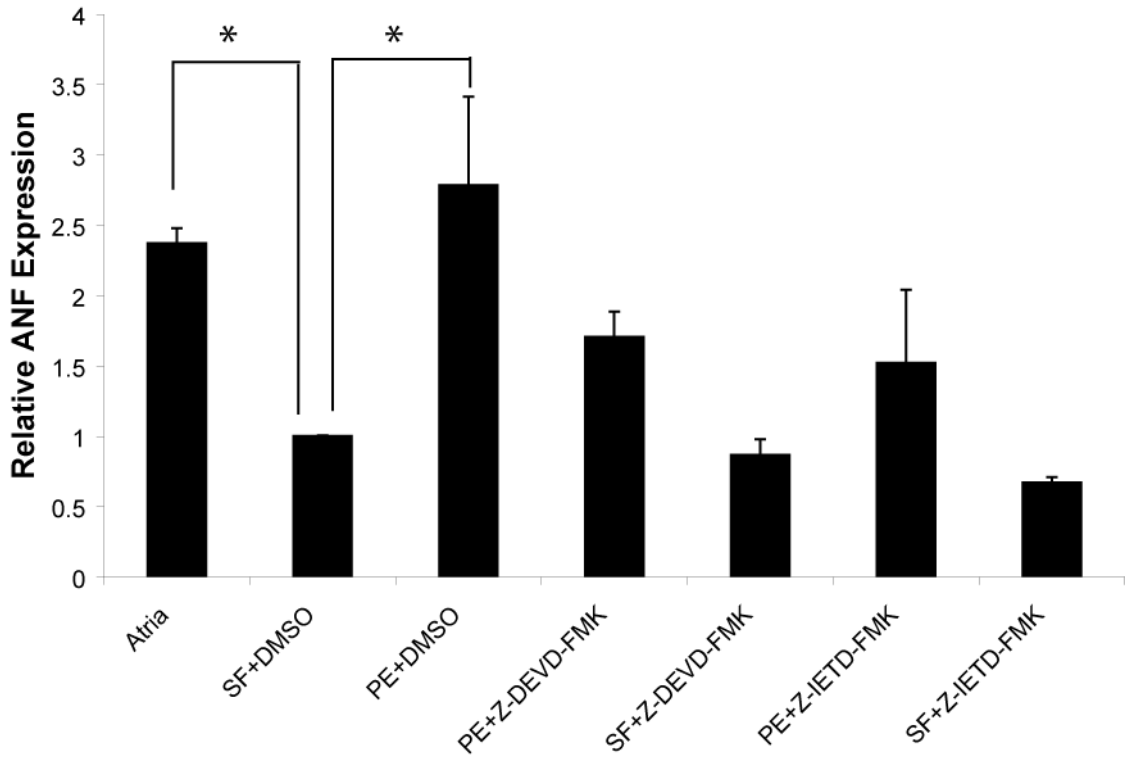

Figure 9: The expression of hypertrophic marker ANF as measured using real-time PCR. PE increased ANF expression by 2.7 fold; Z-DEVD-FMK and Z-IETD-FMK diminished this expression by 50%; the inhibitors did not significantly induce or suppress ANF levels. Atrial tissue was used as a positive control. *P<0.05; n=3.

3.6 Subcellular caspase localization in serum free and hypertrophic conditions

Paradoxically, the global cellular caspase activity did not change in response to hypertrophic agonist treatment, although caspase activity appeared to be required, for the efficient development of cardiomyocyte hypertrophy. As such, the localization of caspase proteins was investigated using fluorescent microscopy under the premise that a focal change in caspase activity, as opposed to a global change in activity levels, may direct the hypertrophic response.

Antibodies against the active forms of caspase-3 and caspase-8 were used in combination with α-actinin to determine the localization of caspases in cardiomyocytes during SF and PE treatments. Quantification of caspase localization was conducted using a cell profiler on AxioVision, as seen in Figure 10 and Figure 11. Localization was determined to be cytosolic when the fluorescence intensity remained constant throughout the cell, nuclear if a co-localization with DAPI was observed, and peri-nuclear if there was an increase in fluorescence around the nucleus, which appeared as spikes in fluorescence using the cell profiler (see Appendix V for additional cell profiles).

Throughout treatment with SF media, active caspase-3 was found primarily within the nucleus (Figure 10). Although caspase-3 was also found to localize to the peri-nuclear area, and also throughout the cytosol, approximately 80% of active caspase-3 was found to be within the nuclei of cardiomyocytes. Following 24 hours of PE treatment, the amount of cytosolic active caspase-3

appeared to be increased by 10%, and nuclear localization was reduced by this amount; however, these results were not found to be significantly different than during serum-free conditions.

In contrast to caspase-3, no nuclear localization of active caspase-8 was observed in either SF conditions or during PE-induced hypertrophy. There was a slight propensity towards peri-nuclear localization, over cytosolic localization, during SF conditions. This trend changed in response to PE treatment such that 70% of active caspase-8 was found throughout the cytosol, with only 30% remaining in the peri-nuclear region (Figure 11). A trend toward the dispersal of caspase-8 activity into the cytosol in response to PE treatment was noted. Following 24 hours of PE treatment, there was significantly more cytosolic caspase-8 activity than per-nuclear activity ($P<0.05$), yet this localization was not found to be significantly different that observed after 24 hours of serum-free conditions. While a significant change in subcellular caspase localization was not observed under the present experimental conditions, caspase-3 or caspase-8 may change localization or level of activity at a time point earlier than measured.

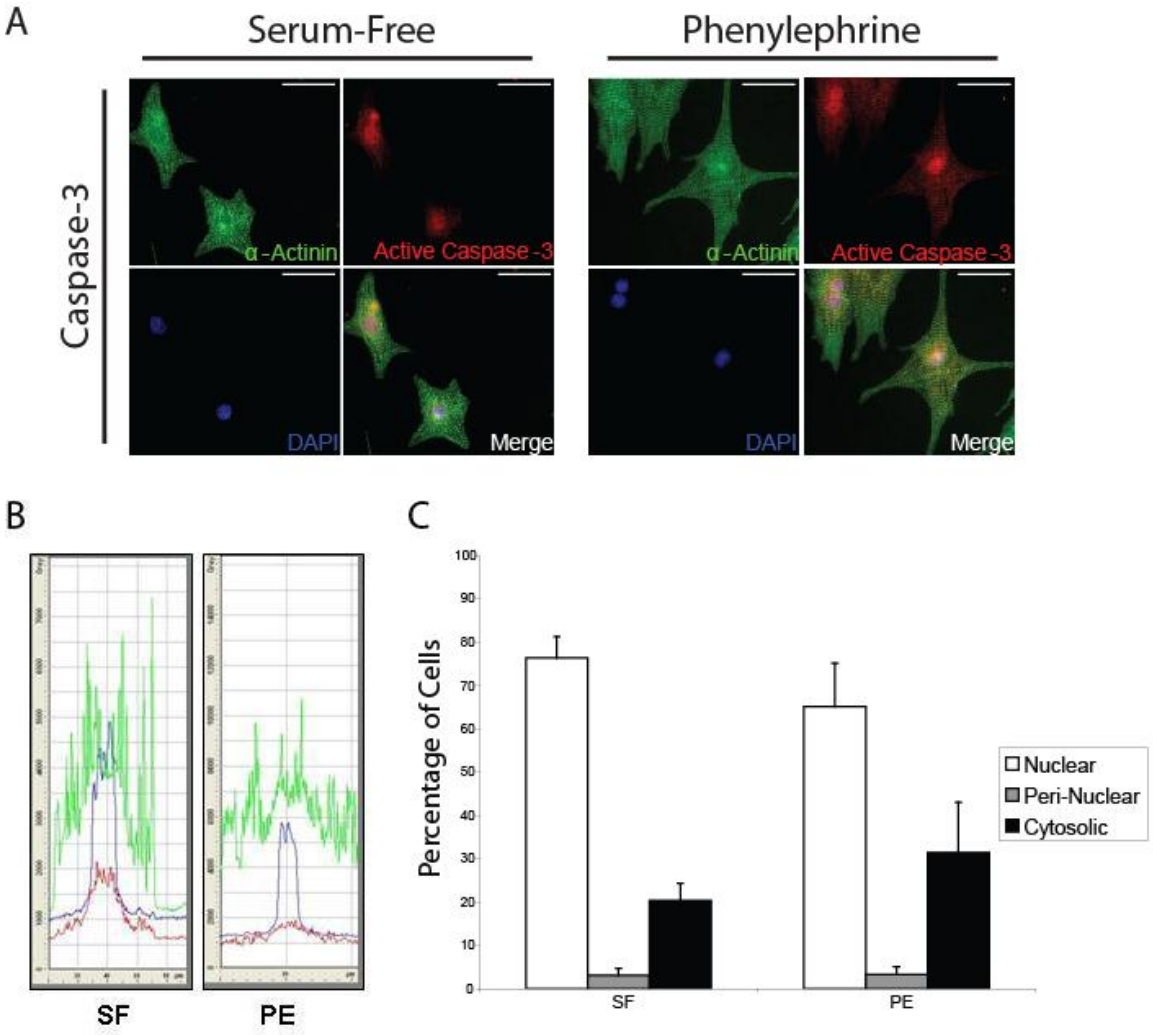

Figure 10: Active caspase-3 localization under SF and hypertrophic conditions as investigated using immunocytochemistry. Cells were stained with α-actinin (green), active caspase-3 (red) and DAPI (blue). a) Active caspase-3 localization within cardiomyocytes was monitored using fluorescence microscopy. b) Localization was analyzed using a cell profiler through AxioVision software; here the x-axis represents the profile or length of the cell and the y-axis represents the fluorescence intensity for each stain mentioned above. c) Caspase localization was quantified as nuclear (white), peri-nuclear (black), or cytosolic (grey); n=3.

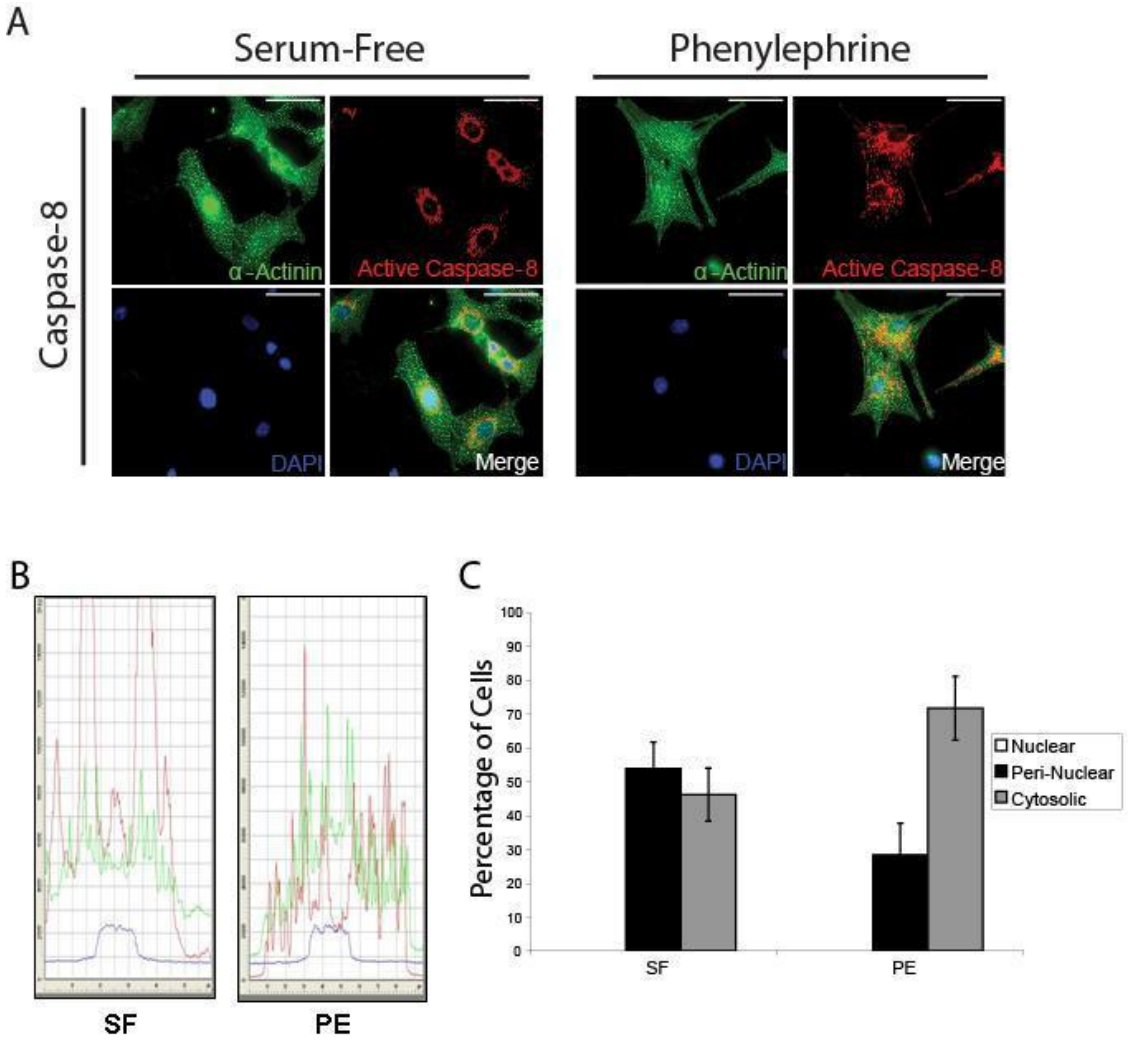

Figure 11: Active caspase-8 localization under SF and hypertrophic conditions as investigated using immunocytochemistry. Cells were stained with α-actinin (green), active caspase-8 (red) and DAPI (blue). a) Active caspase-8 localization within cardiomyocytes was monitored using fluorescence microscopy. b) Localization was analyzed using a cell profiler through AxioVision software; here the x-axis represents the profile or length of the cell and the y-axis represents the fluorescence intensity for each stain mentioned above. c) Caspase localization was quantified as nuclear (white), peri-nuclear (black), or cytosolic (grey); n=3.

CHAPTER 4

Discussion

4.1 Classical role of caspases within cardiomyocytes

The significance of caspase activity within the heart is controversial and is currently an intense area of research. Caspases are typically associated with apoptosis, and caspase activity has been associated with heart failure and the loss of cardiomyocytes within the myocardium in the form of cell death. However, recent evidence suggests that caspases are not only involved in apoptosis, but also cell fate decisions, independent of cell death. Accordingly, the potential involvement of caspases in cardiac hypertrophy is not without foundation and a limited number of studies have implicated caspase activity in this process (Balakumar and Singh, 2006; Haider *et al*., 2002). These studies formed the premise for the current investigation which aimed to determine a cell autonomous role for caspases within cardiomyocytes undergoing hypertrophy *in vitro*.

Historically, caspase expression has been demonstrated in multiple tissue types, including the heart (Van de Craen *et al*., 1997). Caspases were first implicated in heart failure following the discovery of DNA fragmentation in ischemic cardiomyocytes, and in those from patients with dilated cardiomyopathy (Narula *et al*., 1996). Upon closer examination, these cells that had initially been characterized as undergoing cell death, were found to have intact and viable nuclei and failed to induce cleavage of PARP (Haider *et al*., 2002; Narula *et al*., 1999). Therefore, apoptosis was deemed to be incomplete and the possibility that caspases were acting in non-death events was suggested. Additional

investigation into the cross-talk between growth and apoptotic signaling within cardiomyocytes has been conducted with the transcription factor E2F1, whose expression is initially associated with DNA synthesis, but followed closely with apoptosis (Agah *et al*., 1997).

4.2 Caspase inhibition through pharmacological inhibitors minimizes the hypertrophic response in vitro

Caspase-3 and caspase-8 were inhibited simultaneously to eliminate signaling through the extrinsic pathway, and through the final executioner stage of the caspase cascade. Caspase-3 was an interesting protein due to a previous study implicating its requirement during pathological cardiac hypertrophy *in vivo* (Balakumar and Singh, 2006), and because of its function in the cleavage of vital cellular proteins; caspase-8 was investigated due to the cardiac deficiencies seen in the knockout mouse and its integral role in extrinsic caspase signaling. With respect to the intrinsic cascade, caspase-9 was not investigated owing to the fact that cardiomyocytes have been shown previously to struggle with its activation due to decreased levels of Apaf-1 (Samali *et al*., 2007).

Caspase inhibition was first achieved using pharmacological inhibitors, whose mechanism of action will be described in detail in section 4.3. Hypertrophy was first induced using both FBS and PE to ensure substantial growth of the cardiomyocytes and cells were examined throughout 72 hours of treatment to determine the most appropriate time point to investigate in more detail. Following 24 hours in culture, cells had grown significantly, by

approximately 125% compared to untreated cells at time-0. This growth was observed to continue over the course of 72 hours. Inhibition of caspase-3 and -8 resulted in a diminished growth response of only 30% following the same hypertrophic treatment (Figure 5); this trend of an abrogated hypertrophic response with caspase inhibition also continued over 72 hours, however statistical significance was lost after 24 hours. Although FBS has clearly been shown to induce a growth response within cardiomyocytes, the specific factors and proteins within the serum have not been identified and as such, a distinct mechanism through which FBS elicits its effects within the cell during hypertrophy is difficult to quantify. Nonetheless, the observations here collectively support the hypothesis that caspases are involved in cardiac hypertrophy, without subsequent apoptosis.

Due to the fact these initial experiments were not designed to distinguish between the roles of caspase-3 or caspase-8, these experiments were repeated with the separate inhibition of each protease which resulted in a similar blunting of the hypertrophic response, with caspase-3 inhibition significantly abrogating the ability of cardiomyocytes to undergo hypertrophy, and caspase-8 inhibition producing a similar, although non-significant trend. The effectiveness of these chemical inhibitors was also monitored through caspase activity assays which confirmed the inhibition of caspase-3 or caspase-8 specifically to an extent of 80% and 55%, respectively. This information can be combined with the observation that caspase-3 inhibition significantly abrogated the hypertrophic response as measured by both cell area and sarcomeric organization, whereas

caspase-8 inhibition produced a statistically insignificant reduction in hypertrophy. Taken together, this information may suggest that caspase-3 appeared to be required for hypertrophic growth over caspase-8 due to a more efficient inhibition by the pharmacological inhibitor. It would be interesting to investigate the effects of caspase-8 inhibition through either siRNA to gain a more complete genetic knockout.

Cardiomyocytes treated with PE were found to have increased sarcomeric organization, a response that was also less prominent with the addition of caspase-3 or caspase-8 inhibitor (Figure 6). As mentioned above, this reduction in hypertrophic phenotype was also found to be significant with caspase-3 but not caspase-8 inhibition, possibly due to the ability of the inhibitors to effectively inhibit the respective proteases. As some studies have reported methyl ketone caspase inhibitors are able to elicit non-specific effects within the cell (Schotte *et al*., 1999), controlling for treatment with the inhibitors alone ensured the chemical inhibitor did not cause any secondary changes. Although the inhibitors alone did not appear to cause any morphological changes within the cardiomyocytes, further confirmation as to the specificity of the caspase inhibitors was achieved through the use of the molecular inhibitor, p35.

4.3 Functional characteristics of chemical and molecular caspase inhibitors

Due to the challenges pharmacological inhibitors have faced with respect to specificity and potential off-target effects, confirmation of the effects of Z-

DEVD-FMK and Z-IETD-FMK were sought through the use of a molecular inhibitor, p35. Before comparing the results seen with this caspase inhibitor, the molecular characteristics of both types of inhibitors, as well as the functionality of caspase enzymes must be understood in greater detail.

As amino acids serve as the building blocks for proteins, the peptide bonds between residues provide powerful and stable links that under normal conditions remain quite strong. Proteases provide some of the most regulated and controlled means to break such a bond. As described in section 1.6, caspases exist mainly in the form of zymogens within the cells. These zymogens consist of an N-terminal prodomain, as well as large and small subunits, p20 and p10, respectively (Hengartner, 2000). The N-terminal prodomains typically contain the sequences responsible for protein-protein interactions such as the caspase recruitment domain (CARD) and the death effector domain (DED). Caspase activation occurs as a result of cleavage at aspartic acid residues within the prodomain and the linker region between the p20 and p10 subunits (Lamkanfi *et al*., 2002). The active tetrameric protein is a structure containing two p20 and p10 subunits, with the active sites at opposite ends of the protein (Lamfinki *et al*., 2002). In the unprocessed zymogen state, caspases maintain a certain amount of proteolytic ability. Initiator caspase, caspase-8 zymogen is approximately 1% as active as the mature protein, which allows for its autocatalysis upon recruitment to the membrane, whereas active effector caspase, caspase-3 possesses approximately 10 000 times more activity than its zymogen (Lamkanfi *et al*., 2002; Timmer and Salvesen, 2007).

As noted, the mechanism of action for caspases as cysteinyl proteases is exerted by a cysteine residue within the active site of the protein. In addition to the cysteine, caspases possess a histidine residue, which combined, create a catalytic dyad. His237 is able to act as a general base which extracts a proton from Cys285, promoting its nucleophilic ability; the cysteine then creates a tetrahedral intermediate with the substrate through nucleophilic attack on the carbonyl carbon of the scissile bond (Stennicke and Salvensen, 1999).

Caspase recognition sequences are typically exposed along accessible loops of substrate proteins (Mahrus *et al*., 2008). As substrates, both families of inhibitors must contain a caspase recognition sequence. Common to all caspases is the specificity for an aspartic acid residue in what has been deemed the primary specificity position (P_1); the residues occupying P_2-P_4 vary depending on the caspase however P3 is consistently a glutamic acid residue, and the residue on the amino end of the scissile bond, P_1', is generally glycine, serine, or alanine (Timmer and Salvesen, 2007; Salvesen and Riedl, 2008). The cleavage site of a caspase substrate is stabilized through association with corresponding pockets within the caspase, designated as S_1-S_4. The advantage of pharmacological inhibitors is that the recognition sequence can be designed to inhibit a specific caspase. In contrast, the advantage of the molecular inhibitor p35 is that its caspase recognition sequence is broad enough to inhibit most caspases within the cell (Clem, 2001).

Traditionally, cells have maintained the machinery to contain these proteases, and protect the balance between signals from pro-apoptotic proteins by exhibiting their own anti-apoptotic effects; one class of such proteins is the inhibitor of apoptosis proteins (IAPs). IAPs are natural biological inhibitors of apoptosis and caspases, and were initially characterized in baculovirus found to prevent programmed cell death, however since their discovery, homologs of IAPs have been found to be conserved throughout evolution, appearing in organisms from yeast to humans (Wei *et al*., 2008; Clem, 2001). These proteins are characterized by the presence of baculovirus IAP repeat (BIR) domains within the N-terminus, which can bind to the active site of caspases and mediate their inhibition through either sequestering the protein from its substrate, or by promoting its degradation (Wei *et al*., 2008). IAPs are arguably the most studied endogenous inhibitors of apoptosis and caspases; however, in recent years much effort has gone into the specific inhibition of individual caspases which is best done using pharmacological inhibitors.

The inhibitors used in the current investigation were principally chemical inhibitors with a Z motif or benzyloxycarbonyl group on the N-terminus allowing for increased permeability into the cells, and a fluoromethyl ketone (FMK) on the C-terminus which acts as an irreversible inhibitor through alkylation of the cysteine residue in the active site of the caspase (Schotte *et al*., 1999). These inhibitors can be designed for recognition by specific caspases; in the current study, Z-DEVD-FMK was used to specifically inhibit caspase-3, and Z-IETD-FMK was used to inhibit caspase-8. As mentioned in the previous section, there is

redundancy in caspase sequence recognition, and as such, the possibility cannot be excluded that the caspase-3 inhibitor may also inhibit caspase-7 activity. Despite this limitation, these pharmacological inhibitors are the most specific means to chemically inhibit individual caspases and have provided essential tools in the elucidation of the roles of specific caspases in both apoptotic and non-apoptotic settings.

To confirm that the chemical inhibitors were indeed blocking a caspase-mediated signaling pathway, caspase inhibition was also accomplished through infection with a p35 expressing adenovirus. Once inside the cell, p35 acts to competitively inhibit caspases through a suicide mechanism whereby a caspase recognition sequence (D-Q -M-D87↓G) within an accessible reactive site loop (RSL) is recognized by the target caspase and a thioester bond is formed between the active cysteine and the P_1 residue (Fuentes-Prior and Salveesen, 2004; Xu *et al*., 2002; Miller, 1997). Following cleavage of the scissile bond, p35 undergoes a conformational change in which the N-terminus is repositioned near the active site of the caspase, which prevents access of the water molecule and subsequent deacylation of the thioester, and results in an effectively disabled enzyme (Fuienes-Prior and Salvesen, 2004). Furthermore, a cysteine residue within the N-terminus of p35 (Cys-2) is also able to interact with the thioester bond formed between p35 and the inhibited caspase, creating an equilibrium between Asp-87 and the active Cys, and Asp-87 and Cys-2. This reaction ensures the hydrolytic water molecule cannot access the active site and p35 will not undergo circularization (Lu *et al*., 2006).

Like IAP, p35 was initially discovered in baculovirus, however unlike IAPs, currently there are no known mammalian homologs for the p35 gene. P35 is the most extensive inhibitor of caspases known, and inhibits most caspases (Clem, 2001; Fuentes-Prior and Salvesen, 2004). Use of this inhibitor allowed a secondary means to confirm the results observed with pharmacological inhibitors. The p35 gene is best introduced into cardiomyocytes through the use of an adenoviral delivery system. Lipofectamine transfections have proven to be challenging with the cardiomyocyte model, and due to the fact that cardiomyocytes express coxsackie–adenovirus receptors (CARs), adenovirus has become the delivery system of choice. CARs are adhesion molecules that localize to intercalated disks of cardiomyocytes and act as high affinity receptors for adeno virions (Caruso *et al*., 2010; Tan *et al*., 2001).

4.4 Caspase inhibition with p35 minimizes cardiac hypertrophy in vitro

P35 infection was performed at an MOI of 10.0 which was determined to infect 100% of cells without causing apoptosis (see Appendix II). Through expression of a green fluorescent protein (GFP), cells were determined to be successfully infected with the p35 adenovirus. Once again PE treatment was observed to increase the size of cardiomyocytes and this growth was abrogated by the molecular inhibition of caspases. Confirmation of the ability of p35 to inhibit caspases was achieved through caspase activity assays for both caspase-3 and caspase-8 (Appendix II). P35 was found to completely eliminate caspase-3 activity, and dramatically reduce caspase-8 activity to less than 20%. For this

reason, p35 appears to be a superior inhibitor of caspase activity than the pharmacological inhibitors. These results further substantiate the observations obtained with pharmacological inhibition, that there is a requirement for active caspase protease activity within cardiomyocytes during the hypertrophic growth process. Additionally, infection with a GFP-only containing adenovirus confirmed the effects of p35 infection on cell size were specific to caspase inhibition and not a secondary effect of the virus. Cardiomyocytes were observed undergo a minimal hypertrophic growth (9-10%) in response to both p35 and control viral infection without hypertrophic agonist treatment. This growth may be attributed to a cytopathic effect within the cell whereby the virus causes infected cells to swell, and this may occur within the first 24 hours of infection (Cherry, 2004), however the size of these p35 infected cells was not found to be significantly different from that of SF treated cells ($P>0.05$). As such, p35 was determined to be an effective means of both reducing the hypertrophic response in cardiomyocytes, and confirming the specificity of pharmacological caspase inhibition. Due to the fact that p35 does not inhibit a specific caspase, the importance of this result is that it supports the notion that caspases generally, may be somehow required for hypertrophic growth to occur but does not provide further insight into the proteases that may be involved.

4.5 Global cellular caspase activity does not change in response to hypertrophic stimuli

Given the observations that inhibition of caspases minimized the hypertrophic growth of cardiomyocytes, there was a reasonable assumption that

caspase activity may have been altered during the hypertrophic process. To this end, caspase activity was measured at different points throughout the first 24 hours of induced hypertrophy. The caspase activity assay was selected over western blots or immunofluorescent staining for active caspases, as this method provided a readily quantifiable and highly sensitive means to measure caspase activity.

Paradoxically, the results of the caspase activity assays did not suggest that global cellular caspase activity was increased during cardiac hypertrophy. Protein was analyzed from cells following 3, 6, 12, and 24 hours of hypertrophic treatment, however, the activity assays did not indicate any significant change in caspase-3 or caspase-8 activity in response to the treatment. Both the activity of caspase-3, and caspase-8, remained quite low throughout the first 24 hours of hypertrophic induction and was certainly less than that present in apoptotic cells (Figure 8). Because FBS was included in the hypertrophic media initially, it was possible that under these conditions, FBS was not only leading to hypertrophy of the cells, but that it was also influencing their survival (Figure 8a, c). A portion of the caspase activity seen in the serum-free culture may have been that of an apoptotic nature, therefore this activity in hypertrophic cells may have been reduced based on the presence of FBS. To account for this possibility, FBS was removed from the media and the assays were repeated (Figure 8b, d). These assays confirmed that the global cellular caspase activity remained unchanged in response to treatment with hypertrophic agonist phenylephrine alone.

This observation is in contrast to previous reports that demonstrate the non-death function of caspase 3 is associated with elevated proteolytic activity, as in skeletal muscle differentiation (Fernando *et al*., 2002). Given the fact that cardiomyocytes are exceedingly sensitive to perturbations in oxygen content and reactive oxygen species (ROS), these cells may not tolerate the sustained global elevation in caspase activity observed in other cells without engaging a classic apoptosis response. In support of this concept is the observation that cardiomyocytes appear to be resistant to injections with cytochrome c, and have less cellular levels of Apaf-1 which appears to be modulated by a counter upregulation of an IAP in these cells (Potts *et al*., 2005).

The obvious disadvantage of measuring caspase activity obtained from whole cell lysates, is that only global changes in cellular activity will be monitored, and an alteration (if any) in the localization of the protease will not be documented. Furthermore, if caspases are indeed changing localization from the supernatant, to the pelleted component of the lysate, through interaction with a membranous component during hypertrophy, then it is reasonable to assume that a certain amount of caspase activity might be detected in the pelleted fraction and therefore not be measured. A potential strategy to address this limitation would be to analyze both the cytosolic, and membrane fractions of the total lysate. Preliminary experiments however were unsuccessful at investigating this possibility.

Additional approaches to monitoring caspase activity may be useful in future investigations, including a fluorescent resonant energy transfer (FRET) based assay, spatio-temporal activation of caspases (SCAT3) (Takemoto *et al*., 2003), and a fluorescent labeled inhibitor of caspases (FLICA) (Bedner *et al*., 2000). The SCAT3 vector utilizes a cyan fluorescent protein (CFP), linked to a yellow fluorescent protein (YFP) by a series of peptides containing a caspase-3 consensus sequence, DEVD. The premise behind this assay is that active caspase-3 will cleave the linker peptides and upon excitation of CFP, the emission wavelength for YFP will not be detected as the two fluorescent proteins are no longer spatially and temporally connected. Lack of caspase-3 activity would be detected through the presence of FRET within the cells. This assay used in conjunction with confocal microscopy may provide a useful tool for monitoring caspase activity *in* vitro. In contrast, FLICA attempts to label active caspases within whole cells directly using a fluorescent marker. This approach has been met with reports that it is not specific to caspases, and predominantly labels sites other than that of the active sites (Kuzelova *et al*., 2007). Therefore, before this method is employed in cardiomyocytes, the specificity of the label should be further verified.

Despite its limitations, the caspase activity assay as described was optimized in the cardiomyocyte model and was found to be the most reliable method of caspase activity measurement. It remains possible that a novel caspase substrate within the cardiomyocyte may be cleaved preferentially to the fluorogenic substrate, in which case a very modest change in caspase activity

may be overlooked. It also cannot be ignored that without the detection of caspase activity in response to hypertrophic treatment, it is possible that these proteases may not be directly responsible for the hypertrophic response.

4.6 Expression of hypertrophic markers in cells treated with caspase inhibitors

One of the final stages of hypertrophic signaling is the activation of natriuretic peptides and a reversion to the fetal gene program. In turn, activation of these genes inhibits the hypertrophic response by lowering blood pressure and regulating blood volume (Hall, 2004; Kuhn *et al*., 2002; Horio *et al*., 2000). ANF is secreted by the hypertrophic heart and is able to bind to natriuretic peptide receptor type A and guanyl cyclase A, which results in an increase in the production of intracellular cyclic GMP (Hall, 2004; Kuhn *et al*., 2002). As guanyl cyclase A is primarily expressed in the kidneys and vasculature, subsequent production of intracellular cGMP is able to initiate diuresis and vasodilation, which subsequently lowers blood pressure and regulates blood volume (Hall, 2004; Kuhn *et al*., 2002; Horio *et al*., 2000). ANF exerts an additional effect on the hypertrophic cardiomyocytes by inhibiting further agonist-induced hypertrophic growth (Hall, 2004; Calderon *et al*., 1998). The expression of ANF was first monitored using RT-PCR (data not shown). Although a visible increase in ANF expression was observed in response to PE treatment, and appeared to be minimized with the addition of Z-DEVD-FMK, this technique was not able to reliably quantify small changes in expression. Therefore, real-time PCR was employed to quantitatively determine the difference in expression of ANF

following PE treatment, with or without caspase-3 or caspase-8 chemical inhibition. Again the 24 hour time point was examined, and an upregulation of ANF was confirmed in the PE-treated cells and the positive atrial control. With the addition of either caspase-3 or caspase-8 inhibitors, there was a decrease in this upregulation, however, it was not found to be statistically significant. A visible trend exists to suggest that caspases may be acting through a pathway that converges on the upregulation of ANF, however without a significant impact on ANF expression it is also possible that caspases may not directly affect the changes in gene expression associated with PE-induced hypertrophy. Due to the high amount of cross-talk in any given signaling pathway, the inhibition of a single protein may result in the upregulation of another to compensate for the final gene expression, and this may explain why a slight, but not significant decrease in ANF expression was observed. Similarly, the incomplete reduction in caspase-8 activity in response to inhibition may not be sufficient to impact the upregulation of the fetal gene program. These possibilities have not been investigated further, however, use of a pan-caspase inhibitor such as p35 or Z-VAD-FMK may be useful in future investigation into the effects of caspase inhibition on the reactivation of the fetal gene program.

4.7 Caspase localization during hypertrophic growth

Due to the fact that caspase inhibition was noted to have a significant effect on cardiomyocyte growth in response to hypertrophic stimuli, a lack of change in caspase activity during hypertrophy is a paradoxical result. Therefore I hypothesized that a change in the subcellular localization of the active version of

the proteases may contribute to the impact on hypertrophy. At 24 hours post hypertrophic agonist treatment, caspase-3 localization was not found to be significantly different from its localization in SF conditions. There was a noticeable trend toward cytosolic localization, yet the majority of caspase-3 activity remained in the nucleus. In contrast, no caspase-8 activity was seen within the nucleus and there were approximately equal amounts of active caspase-8 localizing around the nucleus and throughout the cytoplasm. In response to PE, caspase-8 had significantly more activity throughout the cytoplasm as compared to the peri-nuclear region; however, this was not significantly different than what was seen in SF conditions. Therefore, although a tendency towards the dispersal of active caspases throughout the cell was observed, these results were inconclusive at the 24 hour time point. It is possible that localization of these proteases may be time sensitive, and a change may be occurring during the earliest phase in the hypertrophy cascade. However, the possibility must be addressed that in the absence of an increase in caspase activity or a decided change in subcellular localization, despite the consistent result that caspase inhibition minimized hypertrophic growth, caspases may not be involved in this aspect of cellular adaptation. Also, the means of analysis used in this experiment depended on inverted microscopy. Perhaps a better approach in the future would be to employ confocal microscopy to determine subcellular localization. A limitation of light microscopy is that it focuses on a single depth within the cell, and is not able to provide a three-dimensional representation of the cell. As such, co-localization studies are difficult to quantify

as the depth of focus may not allow for a comprehensive analysis. Confocal microscopy has overcome this limitation by obtaining optical sections at specific depths within the cell, which can then be combined to produce a three-dimensional image of the cell (Opas, 1999). Using this approach it would be possible to monitor the precise localization of caspase activity within the cell and more accurately determine co-localization with subcellular structures.

Procaspase distribution is typically considered to be cytosolic, yet cleaved substrates of caspase-3 have been found in both the cytosol and the nucleus (Kamada *et al*., 2005). Upon activation, caspase-3 has been shown to translocate into the nucleus. This translocation event requires not only activation of caspase-3, but also substrate recognition (Kamada *et al*., 2005). Based on their study, Kamada *et al*. determined that nuclear translocation was not achieved simply by diffusion of either the zymogen or cleaved caspase, but that translocation was a form of active transport that required a nuclear localizing substrate. It appears logical then, that in the absence of a nuclear-localizing substrate, activated caspases may remain in the cytosol to elicit their effect. The results described in the current investigation were also supported by a study which examined the crosstalk between apoptotic and hypertrophic signaling pathways in cardiomyocytes; here Chatterjee *et al*. also observed predominantly nuclear caspase-3 activity through immunofluorescence with residual activity throughout the cytoplasm in both control and AngII conditions (Chatterjee *et al*., 2010). However, the reports of caspase-3 localization within cardiomyocytes are generally inconsistent, with reports demonstrating nuclear (Chatterjee *et al*.,

2010), cytosolic (Jiang *et al*., 2008), and peri-nuclear activity (Jiang *et al*., 2003). Without a consistent change in subcellular localization it is difficult to determine whether this localization is indeed an aspect of cardiac hypertrophy.

Few studies have investigated the localization of active caspase-8 within cardiomyocytes, and without a known substrate in this context, it is difficult to surmise what caspase-8 may be localizing to around the peri-nuclear region, or in the cytosol. Jiang *et al* reported caspase-8 co-localized with intercalated disks in the cardiomyocyte under normal conditions (Jiang *et al*., 2003). However additional experiments are required to determine whether this phenomenon is specific to a given treatment, or if caspase-8 may be influencing the hypertrophic response with this localization.

Based on this evidence, it is also reasonable to hypothesize that cross-talk may be occurring between caspases and hypertrophic/nuclear signaling pathways. Recently, caspases were found to cleavage-activate calcineurin, which subsequently triggers NFAT activation and nuclear translocation (Muckerjee *et al*., 2001; Santoro *et al*., 1998). Alternatively, caspases may integrate into hypertrophic signaling through cleavage of MEKK1. Indeed, this substrate was identified in response to apoptotic stimuli and was associated with the activation of JNK (Shiah *et al*., 2001). Although cardiac hypertrophy was not analyzed in these studies, it would be interesting to examine whether similar cleavage events are occurring during PE induced cardiac hypertrophy, and

whether caspases concurrently translocate in a fashion to regulate cardiac hypertrophy.

4.8 Conclusions and Future Directions

The current study presents an intriguing body of evidence that caspases-3 and potentially caspase-8 may be required for the physical expansion of cardiomyocytes in response to hypertrophic signaling. Furthermore, it is possible that caspases may be eliciting their effects through signaling pathways leading to the eventual upregulation of ANF, or through a change in subcellular localization. However, due to the currently available models for examining caspases in a non-apoptotic context within cardiomyocytes, a decisive role for these proteins has been difficult to confirm, and as a result it is possible that caspases may not be directly required for this process. Determining a substrate is an obvious subject of future endeavors; however before commencing studies into potential substrates within the pathways, efforts should be made to create a conditional knockout mouse which would allow the deletion of caspase-3 in cardiomyocytes specifically. Such a model would allow the examination of a cell autonomous effect of caspase deletion in cardiomyocytes in response to either pathological or physiological hypertrophy *in vitro* or *in vivo*. Although Balakumar and Singh had attempted a similar study using pharmacological inhibitors, their model had many variables which could not be controlled, specifically the mode of delivery (Balakumar and Singh, 2006).

There are many different avenues in which caspases may be acting to mediate the hypertrophic response, including possible cleavage of HDAC-4 or HDAC-7, an interaction with calcineurin or MEK, or through a novel substrate (McKinsey *et al*., 2000; Scott *et al*., 2008; Chatterjee *et al*., 2010). Although the mechanism has not yet been determined, it cannot be ignored that caspases have emerged as key players in cellular fate decisions, of both apoptotic and non-apoptotic natures. Through the demonstrated roles for caspases in cardiac and skeletal muscle development, and the results shown here, it is no longer unreasonable to suggest that caspases are similarly involved in cardiac hypertrophy. As such, it is important that research continues to be done in this field, as the hypertrophic condition is the leading precursor to heart failure, which has quickly become an epidemic throughout the world. Therapeutic approaches to treat these conditions have made vast improvements over the past few decades; with increased understanding of the signaling mechanisms and molecular underpinnings of cardiac hypertrophy, it is the hope that in the future therapeutic approaches will be able to not only treat, but prevent this condition from occurring.

References

Abdul-Ghani, M., D. Dufort D, R. Stiles, Y. De Repentigny, R. Kothary, and LA Megeney. (2011). Wnt11 promotes cardiomyocyte development by caspase-mediated suppression of canonical Wnt signals. Mol Cell Biol. 31(1):163-178

Adams, JW., AI. Pagel, CK. Means, D. Oksenberg, RC. Armstrong, JH. Brown. (2000). Cardiomyocyte apoptosis induced by Galphaq signaling is mediated by permeability transition pore formation and activation of the mitochondrial death pathway. Circ Res. 87(12):1180-1187.

Agah, R., LA. Kirshenbaum, M. Abdellatiff, LD. Truong, S. Chakraborty, LH. Michael, and MD. Schneider. (1997). Adenoviral delivery of E2F-1directs cell cycle reentry and p53-independent apoptosis in post mitotic adult myocardium in vivo. J Clin Invest. 100:2722-2728.

Aggarwal, B.B. (2003). Signalling pathways of the TNF superfamily: a double-edged sword. Nat Rev Immunol. 3: 745-756.

Anton, R., M. Kühl, and Pandur P. (2007). A molecular signature for the “master” heart cell. Bioassays. 29(5):422-426.

Badorff, C., H. Ruetten, S. Mueller, M. Stahmer, D. Gehrig, F. Jung, C. Ihling, AM. Zeiher, and S. Dimmeler (2002). Fas receptor signaling inhibits glycogen synthase kinase 3 beta and induces cardiac hypertrophy following pressure overload. J Clin Invest. 109(3):373-381.

Balakumar, P., and M. Singh. (2006). The possible role of caspase-3 in pathological and physiological cardiac hypertrophy in rats. Basic Clin Pharmacol Toxicol. 99:418-424.

Banerjee, I., K. Yekkala, T.K. Borg, and T.A. Baudino. (2006). Dynamic interactions between myocytes, fibroblasts, and extracellular matrix. Ann N Y Acad Sci. 1080(1):76-84.

Barry, SP. and PA. Townsend. (2010). What causes a broken heart- molecular insights into heart failure. Int Rev Cell Mol Biol. 284:113-179

Bedner, E., P. Smolewski, P. Amstad, and Z. Daryzkiewicz. (2000). Activation of caspase measured in situ by binding of fluorochrome-labeled inhibitors of caspases (FLICA): correlation with DNA fragmentation. Exp Cell Res. 259(1):308-313.

Braz JC, OF. Bueno, Q. Liang, BJ. Wilkins, YS. Dai, S. Parsons, J. Braunwart, BJ. Glascock, R. Klevitsky, TF. Kimball, TE. Hewett, and JD. Molkentin. (2003). Targeted inhibition of p38 MAPK promotes hypertrophic cardiomyopathy through upregulation of calcineurin-NFAT signaling. J Clin Invest. 110(10):1475-1486.

Calderon, A., CM. Thaik, N. Takahashi, DL. Chang, and WS. Colucci. (1998). Nitric oxide, atrial natriuretic peptide, and cyclic GMP inhibit the growth-promoting effects of norepinephrine in cardiac myocytes and fibroblasts. J Clin Invest. 101(4):812-818.

Carlile, GW., DH. Smith, and M. Wiedmann. (2004). Caspase-3 has a nonapoptotic function in erythroid maturation. Blood. 103(11):4310-4316.

Caruso, L., S. Yuen, J. Smith, M. Husain, and MA. Opavsky. (2010) Crdiomyocyte-targeted overexpression of the coxsackie–adenovirus receptor causes a cardiomyopathy in association with β-catenin signaling. J Mol Cell Cardiol. 48(6):1194-1205.

Chandrashekhar, Y., S. Sen, R. Anway, A. Shuros, and I. Anand. (2004). Long-term caspase inhibition ameliorates apoptosis, reduces myocardial troponin-I cleavage, protects left ventricular function, and attenuates remodeling in rats with myocardial infarction. J Am Coll Cardiol. 43(2):295-301.

Chatterjee, A., SA. Mir, D. Dutta, A. Mitra, K. Pathak, and S. Sarkar. (2010). Analysis of p53 and NF-KB signaling in modulating the cardiomyocyte fate during hypertrophy. J Cell Physiol. [Epub ahead of print].

Cherry, JD. (2004). Adenovirus: Textbook of pediatric infectious diseases 2(5):1843-1845.

Clem, RJ. (2001). Baculovirus and apoptosis: the good, the bad, and the ugly. Cell Death Differ. 8(2):137-143.

Communal, C., M. Sumandea, P. de Tombe, J. Narula, RJ. Solaro, and RJ. Hajjar. (2002). Functional consequences of caspase activation in cardiac myocytes. Proc Natl Acad Sci USA. 99(9):6252-6256.

Cory, S. (1998). Cell death throes. Proc Natl Acad Sci. 95:12077-12079.

Derynck, R. and Akhurst, R.J. (2007). Differentiation plasticity regulated by TGF-β family proteins in development and disease. Nat Cell Biol. **9:**1000-1004.

Dolmetsch, RE., RS. Lewis, CC. Goodnow, and JI. Healy. (1997). Differential activation of transcription factors induced by Ca2+ response amplitude and duration. Nature. 386(6627):855-858.

Dorn, GW. (2007). The fuzzy logic of physiological cardiac hypertrophy. Hypertension. 49(5):962-970.

Earnshaw, W.C., LM. Martins, and SH. Kaufmann. (1999). Mammalian caspases: Structure, activation, substrates and functions during apoptosis. Annu Rev Biochem. 68: 383-424.

Fielitz J, MS. Kim, JM. Shelton, X. Qi, JA. Hill, JA. Richardson, R. Bassel-Duby, and Olson EN. (2008). Requirement for protein kinase D1 for pathological cardiac remodeling. Proc Natl Acad Sci USA. 105(8):30593063.

Fernando, P., JF. Kelley, K. Balazsi, R. Slack, and LA. Megeney. (2002). Caspase 3 activity is required for skeletal muscle differentiation. Proc Natl Acad Sci USA. 99(17):11025-11030.

Fernando, P and Megeney, L.A. (2007). Is caspase-dependent apoptosis only cell differentiation taken to the extreme? FASEB J. 21: 8-17,

Feuntes-Prior, P. and Salvesen, G. (2004). The protein structures that shape caspase activity, specificity, activation and inhibition. Biochem J. 384(Pt 2): 201-232.

Fischer, U., R U Jänicke, and K. Schulze-Osthoff. (2003). Many cuts to ruin: a comprehensive update of caspase substrates. Cell Death and Differentiation. 10:76-100.

Frey, N. and EN. Olson. (2003). Cardiac hypertrophy: the good, the bad, and the ugly. Annu Rev Physiol. 65:45-79.

Gregorio, CC., and Antin, PB. (2000). To the heart of myofibril assembly. Trends Cell Biol. 10(9):355-362.

Haider, N., N. Narula, and J. Narula. (2002). Apoptosis in heart failure represents programmed cell survival, not death, of cardiomyocytes and likelihood of reverse remodeling. J Card Fail. 8(6):S512-S517.

Hall, C. (2004). Essential biochemistry and physiology of (NT-pro)BNP. Eur J Heart Fail. 6(3):257-260.

Heineke, J. and Molkentin, JD. (2006). Regulation of cardiac hypertrophy by intracellular signaling pathways. Nat Rev Mol Cell Biol. 7(8):589-600.

Hengartner, MO. (2000). The biochemistry of apoptosis. Nature. 407:770-776.

Hill, JA. and Olson, EN. (2008). Cardiac plasticity. N Engl J Med. 358(13):1370-1380.

Horio, T., T. Nishikimi, F. Yoshihara, H. Matsuo, S. Takishita, and K. Kangawa. (2000). Inhibitory regulation of hypertrophy by endogenous atrial natriuretic peptide in cultured cardiac myocytes. Hypertension. 35(1 Pt 1):19-24.

Huang, W., J. Fileta, I. Rawe, J. Qu, and CL. Grosskreutz. (2010). Calpain activation in experimental glaucoma. Invest Ophthalmol Vis Sci. 51(6):3049-3054.

Hudek, SB., GE. Taffet, MD. Schneider, and DL. Mann. (2007). TNF provokes cardiomyocyte apoptosis and cardiac remodeling through activation of multiple cell death pathways. J Clin Invest. 117(9):2692-2701.

Jiang L, Y. Huang, S. Hunyo, and CG. dos Remedios. (2003). Cardiomyocyte apoptosis is associated with increased wall stress in chronic failing left ventricle. Eur Heart J. 24(8)742-751.

Jiang, CM., LP. Han, HZ. Li, YB. Qu, ZR. Zhang, R. Wang, CQ. Xu, and WM. Li. (2008). Calcium-sensing receptors induce apoptosis in cultured neonatal rat ventricular cardiomyocytes during simulated ischemia/reperfusion. Cell Biol Int. 32(7):792-800.

Kamada S, U. Kikkawa, Y. Tsujimoto, and T. Hunter. (2005). Nuclear translocation of caspase-3 is dependent on its proteolytic activation and recognition of a substrate-like protein(s). J Biol Chem. 280(2)857-860.

Kang, TB., T. Ben-Moshe, EE. Varfolomeev, Y. Pewzner-Jung, N. Yogev, A. Jurewicz, A. Waisman, O. Brenner, R. Haffner, E. Gustafsson, P. amakrishnan, T. Lapidot, and D. Wallach. (2004). Caspase 8 serves both apoptotic and nonapoptotic roles. J Immunol. 173(5):2976- 2984.

Kang, SJ., S. Wang, K. Kuida, J. Yuan. (2002). Distinct downstream pathways of caspase-11 in regulating apoptosis and cytokine maturation during septic shock response. Cell Death Differ. 9(10): 1115-1125.

Kim, Y., D. Phan, E. van Rooij, DZ. Wang, J. McAnally, X. Qi, JA. Richardson, JA. Hill, R. Bassel-Duby, and EN. Olson. (2008). The MEF2D transcription factor mediates stress-dependent cardiac remodeling in mice. J Clin Invest. 118(1):124-132.

Kuhn, M., R. Holtwick, HA. Baba, JC. Perriard, W. Schmitz, and E. Ehler. (2002). Progressive cardiac hypertrophy and dysfunction in atrial natriuretic peptide receptor (GC-A) deficient mice. Heart. 87(4):368-374.

Kuzelova, K., D. Grebenova, Z. Hrkal. (2007). Labeling of apoptotic JURL-MK1 cells by fluorescent caspase-3 inhibitor FAM-DEVD-fmk occurs mainly at site(s) different from caspase-3 active site. Cytometry A. 71(8):605-611.

Lamkanfi, M., W. Declercq, M. Kalai, X. Saelens and P. Vandenabeele. (2002). Alice in caspase land. A phylogenetic analysis of caspases from worm to man. Cell Death Differ. 9(4):358-361.

Larsen BD, S. Rampalli, LE. Burns, S. Brunette, FJ. Dilworth, and LA. Megeney. (2010). Caspase 3/caspase-activated DNase promote cell differentiation by inducing DNA strand breaks. Proc Natl Acad Sci USA. 107(9):4230-4235.

Li. J., WM. Brieher, ML. Scimone, SJ. Kang, H. Zhu, H. Yin, UH. Von Andrian, T. Mitchison, and J. Yuan. (2007). Caspase-11 regulates cell migration by promoting Aip1-Cofilin-mediated actin depolymerization. Nat Cell Biol. 9(3):276-286.

Lu, M., T. Min, D. Eliezer, and H. Wu. (2006). Native chemical ligation in covalent caspase inhibition by p35. Chem Biol. 13(2):117-122.

Mahrus, S., JC. Trinidad, DT. Barkan, A. Sali, AL. Burlingame, and JA. Wells. (2008). Global sequencing of proteolytic cleavage sites in apoptosis by specific labeling of protein N termini. Cell. 134(5):866-876.

Martinon, F., J. Tschopp. (2007). Inflammatory caspases and inflammasomes: master switches of inflammation. Cell Death Differ. 14:10-22.

McKinsey TA, CL. Zhang, J. Lu, and EN. Olson. (2000). Signal-dependent nuclear export of a histone deacetylase regulates muscle differentiation. Nature. 408(6808):106-111.

McIlroy, D., Sakahira, H., Talanian, R.V., Nagata, S. (1999). Involvement of caspase 3-activated DNase in internucleosomal DNA cleavage induced by diverse apoptotic stimuli. Oncogene. 18(31): 4401-4408.

McMullen, JR., F. Amirahmadi, EA. Woodcock, M. Schinke-Braun, RD. Bouwman, KA. Hewitt, JP. Mollica, L. Zhang, Y. Zhang, T. Shioi, A. Buerger, S. Izumo, PY. Jay, and GL. Jennings. (2007). Protective effects of exercise and phosphoinositide 3-kinase (p110alpha) signaling in dilated and hypertrophic cardiomyopathy. Proc Natl Acad Sci USA. 104(2):612-617.

McMullen, JR. and Jennings, GL. (2007). Differences between pathological and physiological cardiac hypertrophy: novel therapeutic strategies to treat heart failure. Clin Exp Pharmacol Physiol. 34(4):255-262.

McMullen, JR., T. Shioi, L. Zhang, O. Tarnavski, MC. Sherwood, PM. Kang, and S. Izumo. (2003). Phosphoinositide 3-kinase (p110alpha) plays a critical role for the induction of physiological, but not pathological, cardiac hypertrophy. Proc Natl Acad Sci USA. 100(21):12355-12360.

Miller, LK. (1997). Baculovirus interaction with host apoptotic pathways. J Cell Physiol. 173:178-182.

Milligan, C.E. and Schwartz, L.M. (1997). Programmed cell death during animal development. Br Med Bull. 52(3):570-590.

Molkentin, JD., JR. Lu, CL. Antos, B. Markham, J. Richardson, J. Robbins, SR. Grant, and EN. Olson. (1998). A calcineurin-dependent transcriptional pathway for cardiac hypertrophy. Cell. 93(2):215-228.

Mukerjee, N., KM. McGinnis, ME. Gnegy, and KK. Wang. (2001). Caspase-mediated calcineurin activation contributes to IL-2 release during T cell activation. Biochemical and Biophysical Research Communications. 285(5):1192-1199.

Narula, J., N. Haider, and R. Virmani. (1996). Apoptosis in myocytes in end-stage heart failure. N Engl J Med. 335:1182-1189.

Narula, J., P. Pandey, E. Arbustini, N. Haider, N. Narula, FD. Kolodgie, B. Dal Bello, MJ. Semigran, A. Bielsa-Masdeu, GW. Dec, S. Israels, M. Ballester, R. Virmani, S. Saxena, S. Kharbanda. (1999). Apoptosis in heart failure: release of cytochrome c from mitochondria and activation of caspase-3 in human cardiomyopathy. Proc Natl Acad Sci USA. 96(14):8144-8149.

Obeng, EA., LH. Boise. (2005). Caspase-12 and caspase-4 are not required for caspase-dependent endoplasmic reticulum stress-induced apoptosis. The J Biol Chem. 280: 29578-29587.

Okuyama, R., BC. Nguyen, C. Talora, E. Ogawa, A. Tommase di Vigano, M. Lioumi, G. Chiorino, H. Tagami, M. Woo, and GP. Dotto. (2004). High commitment of embryonic keratinocytes to terminal differentiation through a Notch1-caspase 3 regulatory mechanism. Dev Cell. 6(4):551-562.

Olson, EN. (2006). Gene regulatory networks in the evolution and development of the heart. Science. 313(5795:1922-1927.

Olson, EN. (2004). A decade of discoveries in cardiac biology. Nat Med. 10(5):467-474

Opas, M. (1999). Fluorescence tracing of intracellular proteins. Biotech Histochem. 74(6):294-310

Pandur, P., M. Lasche, LM. Eisenberg, and M. Kuhl. (2002). Wnt-11 activation of non-canonical Wnt signaling pathway is required for cardiogenesis. Nature. 418:636-641.

Potts, MB., AE. Vaughn, H. McDxonough, C. Patterson, and M. Deshmukh. (2005). Reduced Apaf-1 levels in cardiomyocytes engage strict regulation of apoptosis by endogenous XIAP. J Cell Biol. 171(6):925-930.

Puig, B., A. Tortosa, and I. Ferrer. (2001). Cleaved caspase-3, caspase-7 and poly (ADP-ribose) polymerase are complementary but differentially expressed in human medulloblastomas. Neurosci Lett. 306(1-2):85-88.

Revankar, CM., CM. Vines, DF. Cimino, and ER. Prossnitz. (2004). Arrestins block G protein-coupled receptor-mediated apoptosis. J Biol Chem. 279(23):24578-24584.

Riento, K., and Ridley, AJ. (2003). Rocks: multifunctional kinases in cell behaviour. Nat Rev Mol Cell Biol. 4(6):446-456.

Sakamaki, K., T. Inoue, M. Asano, K. Sudo, H. Kazama, J. Sakagami, S. Sakata, M, Ozaki, S. Nakamura, S. Toyokuni, N. Osumi, Y. Iwakura, and S. Yonehara. (2002). Cell Death Differ. 9:1196-1206.

Salmena, L., B. Lemmers, A. Hakem, E. Matysiak-Zablocki, K. Murakami, PY. Au, DM. Beny, L. Tamblyn, A. Shehabeldin, E. Migon, A. Wakeham, D. Bouchard, WC. Yeh, JC. McGlade, PS. Ohashi, and R. Hakem. (2003). Essential role for caspase 8 in T-cell homeostasis and T-cell mediated immunity. Genes Dev. 17(7):883-895.

Salvesen, GS. and Riedl, SJ. (2008). Caspase mechanisms. Adv Exp Med Biol. 615:13-23.

Samali, A., M. O'Mahoney, J. Reeve, S. Logue, E. Szegezdi, H=J. McMahon, and HO. Fearnhead. (2007). Identification of an inhibitor of caspase activation from heart extracts; ATP blocks apoptosome formation. Apoptosis. 12(3):465-474.

Sanna, B., OF. Bueno, YS. Dai, BJ. Wilkins, and JD. Molkentin. (2005). Direct and indirect interactions between calcineurin-NFAT and MEK1-extracellular signal-regulated kinase 1/2 signaling pathways regulate cardiac gene expression and cellular growth. Mol Cell Biol. 25(3):865-878.

Santoro, MF., RR. Annand, MM. Robertson, YW. Peng, MJ. Brady,JA. Mankovich, MC. Hackett, T. Ghayur, G. Walter, WW. Wong, and DA. Giegel. (1998). Regulation of protein phosphatase 2A activity by caspase-3 during apoptosis. J Biol Chem. 273:13119-13128.

Schotte, P., W. Declercq, S. Van Huffel, P. Vandenabeele, and R. Beyaert. (1999). Non-specific effects of methyl ketone peptide inhibitors of caspases. FEBS Lett. 44(1):117-121/

Schwerk, C., and K. Schulze-Osthoff. (2003). Non-apoptotic functions of caspases in cellular proliferation and differentiation. Biochem Pharmacol. 66(8):1453-1458.

Scott, FL., GJ. Fuchs, SE. Boyd, JB. Denault, CJ. Hawkins, F. Dequiedt, and GS. Salvesen. (2008). Caspase-8 cleaves histone deacetylase 7 and abolishes its transcription repressor function. J Biol Chem. 283(28):19499-19510.

Shiah, SG., SE. Chuang, and ML. Kuo. (2001). Involvement of Asp-Glu-Val-Asp-directed caspase-mediated mitogen-activated protein kinase kinase 1 cleavage, c-Jun N-terminal kinase activation, and subsequent Bcl-2 phosphorylation for paclitaxel-induced apoptosis in HL-60 cells. Mol Pharmacol. 59(2):254-262.

Siegel, R.M. (2006). Caspases at the crossroads of immune-cell life and death. Nat RevImmunol. 6: 308-317.

Souders, CA., SLK. Bowers, and TA. Baudino. (2009). Cardiac fibroblast: The renaissance cell. Circ Res. 105:1164-1176.

Srivastava D, and Olson EN. (2000). A genetic blueprint for cardiac development. Nature. 407(6802):221-226.

Stennicke, HR. and Salvesen, GS. (1999). Catalytic properties of the caspases. Cell Death Differ. 6(11):1054-1059.

Sugden, PH. (1999). Signaling in myocardial hypertrophy: Life after calcineurin? Circ Res. 84:633-646.

Takemoto, K., T. Nagai, A. Miyawaki, and M. Miura. (2003). Spatio-temporal activation of caspase revealed by indicator that is insensitive to environmental effects. J Cell Biol. 160(2):235-243.

Talanian, RV., C. Quinlan, S. Trautz, MC. Hackett, JA. Mankovich, D. Banach, T. Ghavur, KD. Brady, and WW. Wong. (1997). Substrate specificities of caspase family proteases. J Biol Chem. 272:9677-9682.

Tan, PK., AI. Michou, JM. Bergelson, M. Cotton. (2001). Defining CAR as a cellular receptor for the avian adenovirus CELO using a genetic analysis of the two viral fibre proteins. J Gen Virol. 82:1465-1472.

Timmer, JC. and GS. Salvesen. (2007). Caspase substrates. Cell Death Differ. 14(1):66-72.

Van de Craen, M., P. Vandenabeele, W. Declercq, I. Van den Brande, G. Van Loo, F. Molemans, P. Schotte, W. Van Criekinge, R. Beyaert, and W. Fiers. (1997). Characterization of seven murine caspase family members. FEBS Lett. 403(1):61-69.

Varfolomeev, EE., M. Schuchmann, V. Luria, N. Chiannilkulchai, JS. Beckmann, IL. Mett, D. Rebrikoy, VM. Brodianski, OC. Kemper, O. Kollet, T. Lapidot, D. Soffer, T. Sobe, KB. Avraham, T. Goncharov, H. Holtmann, P. Lonai, and D. Wallach. (1998). Targeted disruption of the mouse Caspase 8 gene ablates cell death induction by the TNF receptors, Fas/Apo1, and DR3 and is lethal prenatally. Immunity. 9(2):267-276.

Vitale, G., M. Galderisi, A. Colao, P. Innelli, G. Guerra, E. Guerra, F Jr. Orio, A. Soscia, O, De Divitiis, and G. Lombardi. (2008). Circulating IGF-I levels are associated with increased biventricular contractility in top-level rowers. Clin Endocrinol. 69(2):231-236.

Wehrens, X.H.T., S.E. Lehnart, S. Reiken, R. van der Nagel, R. Morales, J. Sun, Z. Cheng, S. Deng, L.J. Windt, D. W. Landry, and A.R. Marks. (2005). Enhancing calstabin binding to ryanodine receptors improves cardiac and skeletal muscle function in heart failure. Proc Natl Acad Sci USA. 102(27):9607-9612

Wei, Y., T.Fan, and M. Yu. (2008). Inhibitor of apoptosis proteins and apoptosis. Acta Biochimi Biophys Sin. 40(4):278-288.

Yarbrough, WM., R. Mukherjee, GP. Escobar, JA. Sample, JE. McLean, KB. Dowdy, JW. Hendrick, WC. Gibson, AE. Hardin, JT. Mingoia, PC. White, A. Stiko, RC. Armstrong, FA. Crawford, and FG. Spinale. (2003). Pharmacologic inhibition of intracellular caspases after myocardial infarction attenuates left ventricular remodeling: A potentially novel pathway. J Thorac Cardiovasc Surg. 126:1892-1899.

Yarbrough, WM., R. Mukherjee, RE. Stroud, EC. Meyer, GP. Escobar, JA. Sample, JW. Hendrick, JT. Mingoia, and FG. Spinale. (2010). Caspase inhibition modulates left ventricular remodeling following myocardial infarction through cellular and extracellular mechanisms. J Cardiovasc Pharmacol. 55(4):408-416.

Xu, G. RL. Rich, C. Steegborn, T. Min, Y. Huang, DG. Myszka, and H. Wu. (2002). Mutational analysis of the p35-caspase interaction : A bowstring kinetic model of caspase inhibition by p35. J Biol Chem. 270:5455-5461.

Zak, R. (1973). Cell proliferation during cardiac growth. Am J Cardiol. 31(2):211-219.

Zhang, CL. TA. McKinsey, S. Chang, CL. Antos, JA. Hill, and Olson EN. (2002). Class II histone deacetylases act as signal-responsive repressors of cardiac hypertrophy. Cell. 110(4):479-488.

APPENDIX I

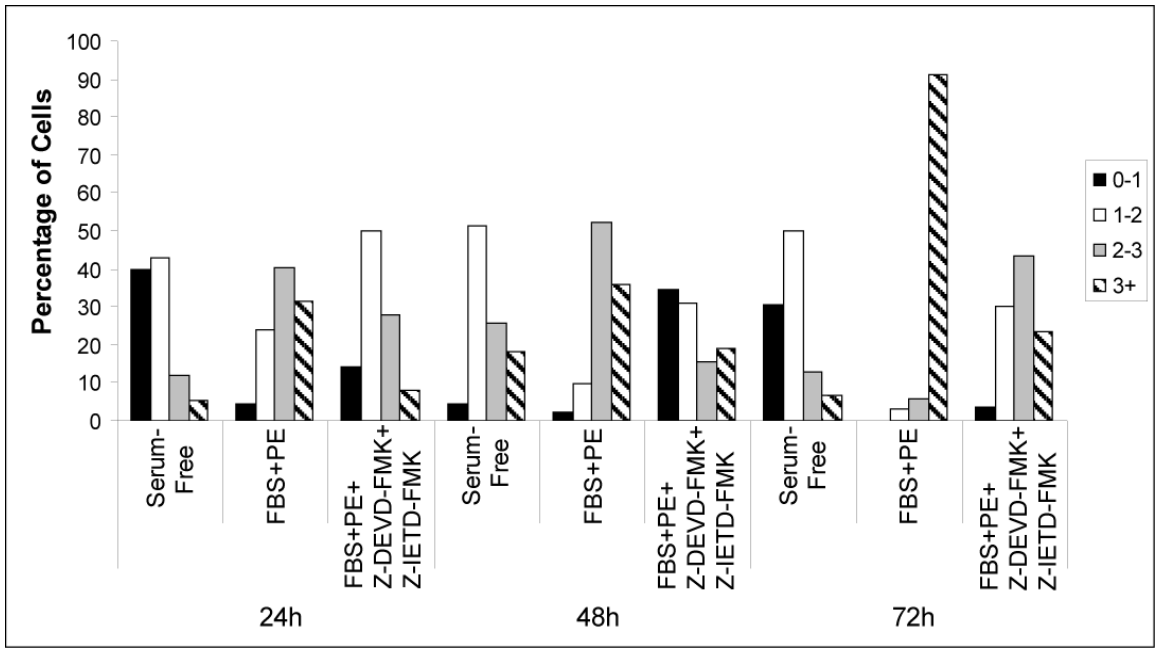

Figure S. 1: Representation of the cell size distributions per given treatment. Cell sizes were placed into bins, relative to the average cell size at time-0. Cells that were the same size or smaller than that at time-0 were placed in the 0-1 (fold growth) bin (black); cells that grew up to two times in size were placed in the 1-2 bin (white); cells that grew two to three times their initial size are represented in the 2-3 bin (grey), and the proportion of cells that experienced greater than threefold growth are represented in the 3+ bin (striped).

APPENDIX II

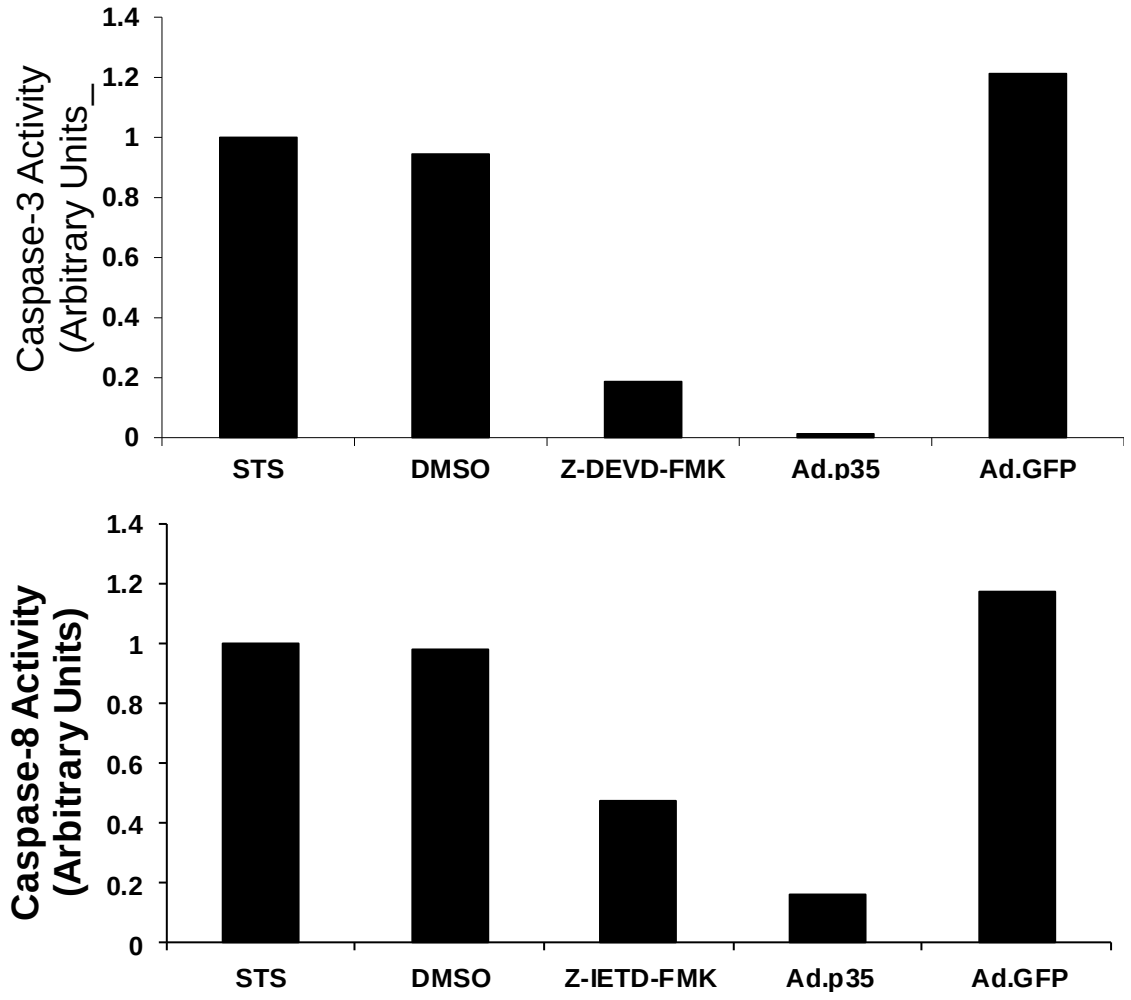

Figure S. 2: Effectiveness of caspase inhibitors. Caspase-3 and caspase-8 were activated through incubation in 1 μM staurosporine (STS) for four hours. The vehicles only for caspase inhibition (DMSO and Ad.GFP) were not found to inhibit caspase activity themselves. 20 μM Z-DEVD-FMK was found to inhibit caspase-3 by 80% and p35 completely eliminated this activity. 20 μM Z-IETD-FMK decreased caspase-8 activity by 55%, and p35 inhibited this activity by 80%.

APPENDIX III

A

MOI = 10 infectious particles per cell (10ipu/cell)

No. cells per well = $2.5x10^3$

IPU = $2.5x10^3$ cells (10 ipu/cell)
= $2.5x10^4$ infectious particles

Volume p35Ad = $2.5x10^4$ particles / [$3.608x10^{10}$ ipu/mL]
=0.0006929 µL/plate

B

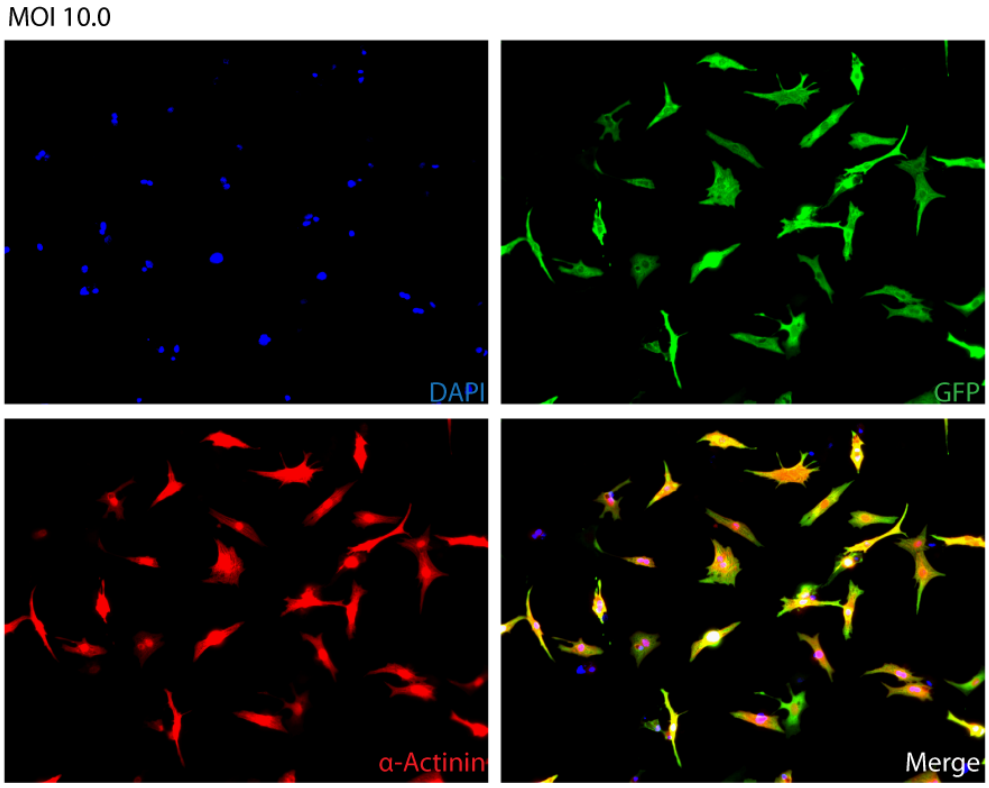

Figure S. 3: Multiplicity of Infection for p35Ad. a) Calculation for the determination of Multiplicity of Infection. b) Cardiomyocytes were infected with p35Ad at MOIs ranging from 0.1-100. Shown here is an MOI of 10.0 which was found to have a 100% rate of infection and did not induce apoptosis within the cells.

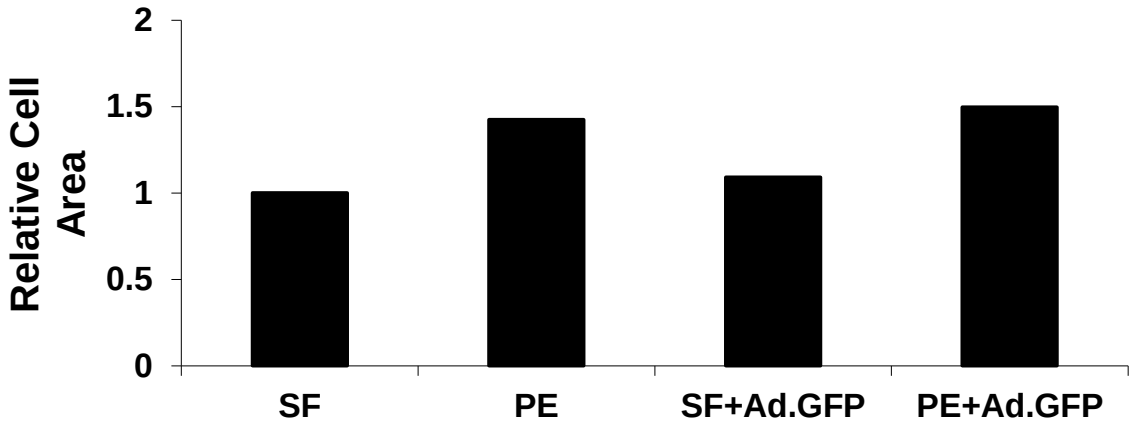

Figure S. 4: Effect of Ad.GFP on cardiomyocyte size. 100um phenylephrine (PE) induced a 45% increase in cell area compared to serum-free (SF) treated cells. The presence of the GFP containing adenovirus did not affect cardiomyocyte size in either SF or PE conditions. n=1.

APPENDIX IV

Processing of real-time Polymerase Chain Reaction data

All samples were run in duplicate

ANF expression values were analyzed relative to internal housekeeping gene, GAPDH

Results were further normalized to a reference sample, serum-free treated cells.

Cycle thresholds (Cts) were set within the linear portion of the curve, at a point in which the duplicate samples were closest in value. This value represents the cycle at which fluorescence was increased above background levels.

Table S. 1: Example of analysis for real-time PCR

Treatment	Ct_{ANF}	Ct_{GAPDH}	ΔCT	ΔΔCT	$2^{-\Delta\Delta CT}$
Serum-Free	23.57	17.96	5.61	0	1
100μM PE	18.64	14.65	5.61	-1.62	3.086
100μM PE + 20μM Z-DEVD-FMK	18.89	14.31	5.61	-1.03	2.046
20μM Z-DEVD-FMK	22.445	16.205	5.61	0.63	0.646
100μM PE + 20μM Z-IETD-FMK	19.125	14.775	5.61	-1.26	2.396
20μM Z-IETD-FMK	22.555	16.32	5.61	0.625	0.648

APPENDIX V

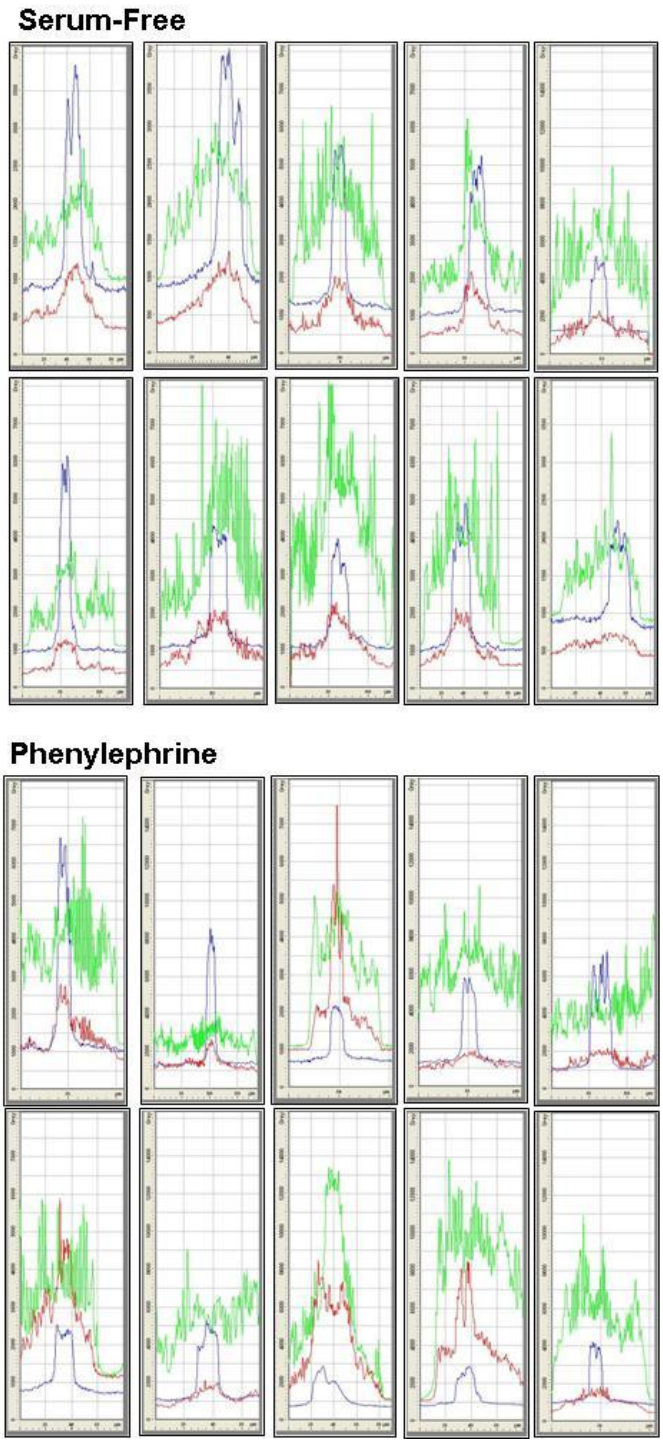

Figure S. 5: Representative cell profiles of caspase-3 localization taken from cardiomyocytes using AxioVision software. Cardiomyocytes were stained with α-actinin (green), DAPI (blue) and active-caspase-3 (red). The x-axis represents the length, or profile of a cell, and the y-axis represents the amount of fluorescence detected.

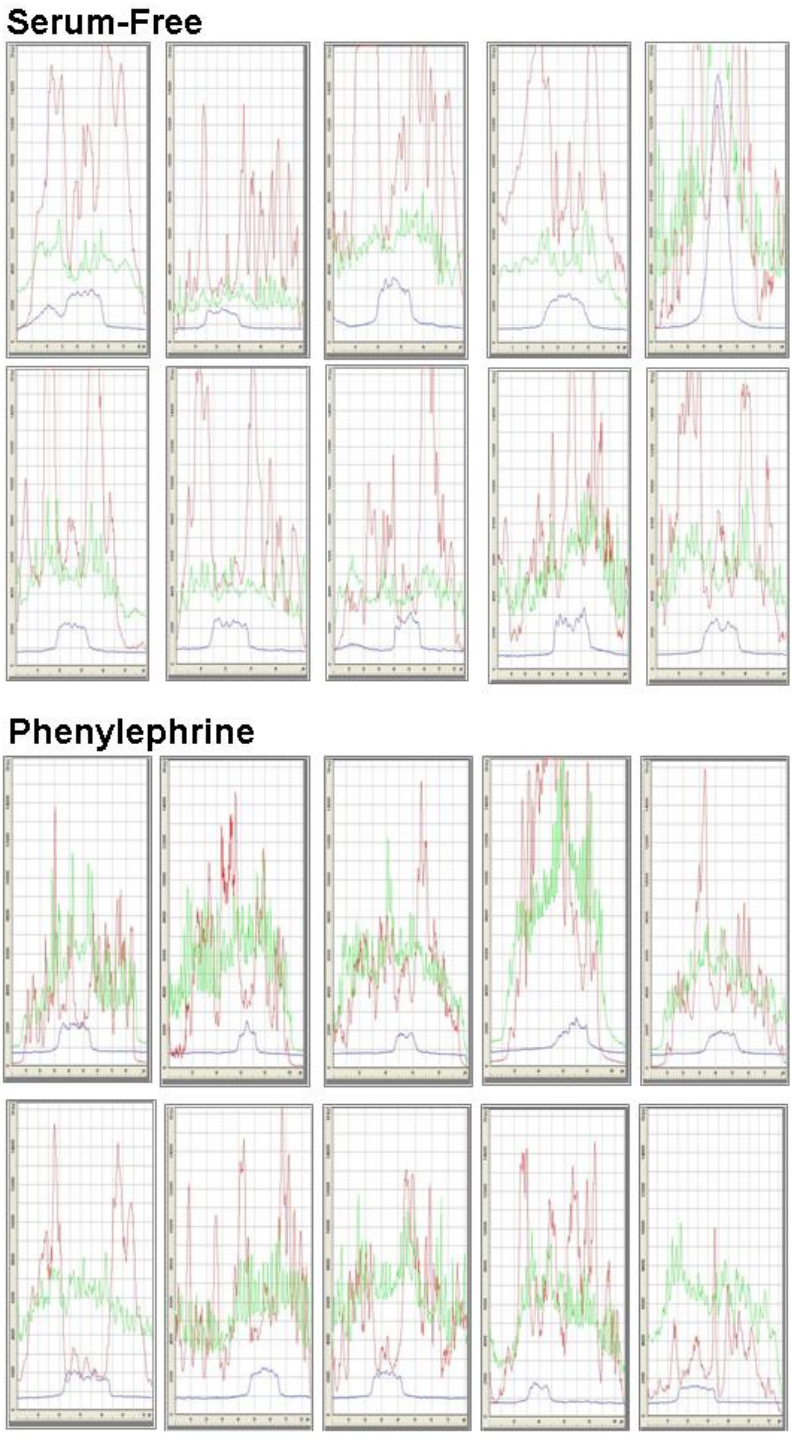

Figure S. 6: Representative cell profiles of caspase-8 localization taken from cardiomyocytes using AxioVision software. Cardiomyocytes were stained with α-actinin (green), DAPI (blue) and active-caspase-8 (red). The x-axis represents the length, or profile of a cell, and the y-axis represents the amount of fluorescence detected.